nature immunology

An essential role for the IL-2 receptor in T_{reg} cell function

Takatoshi Chinen[1,2,10], Arun K Kannan[3,9,10], Andrew G Levine[1,2], Xiying Fan[1,2], Ulf Klein[4–6], Ye Zheng[7], Georg Gasteiger[1,2,8], Yongqiang Feng[1,2], Jason D Fontenot[3,9] & Alexander Y Rudensky[1,2]

Regulatory T cells (T_{reg} cells), which have abundant expression of the interleukin 2 receptor (IL-2R), are reliant on IL-2 produced by activated T cells. This feature indicates a key role for a simple network based on the consumption of IL-2 by T_{reg} cells in their suppressor function. However, congenital deficiency in IL-2R results in reduced expression of the T_{reg} cell lineage–specification factor Foxp3, which has confounded experimental efforts to understand the role of IL-2R expression and signaling in the suppressor function of T_{reg} cells. Using genetic gain- and loss-of-function approaches, we found that capture of IL-2 was dispensable for the control of $CD4^+$ T cells but was important for limiting the activation of $CD8^+$ T cells, and that IL-2R-dependent activation of the transcription factor STAT5 had an essential role in the suppressor function of T_{reg} cells separable from signaling via the T cell antigen receptor.

© 2016 Nature America, Inc. All rights reserved.

Regulatory T cells (T_{reg} cells) that express the transcription factor Foxp3 restrain immune responses to self and foreign antigens[1–3]. T_{reg} cells have abundant expression of the interleukin 2 receptor α-chain (IL-2Rα; CD25) but are unable to produce IL-2. IL-2 binds with low affinity to IL-2Rα or to heterodimers of the common γ-chain (γ_c; CD132) and IL-2Rβ (CD122), but receptor affinity increases ~1,000-fold when these three subunits collectively interact with IL-2 (ref. 4). IL-2 and the transcription factor STAT5, a key target downstream of JAK kinases associated with IL-2R, are indispensable for inducing the expression of Foxp3 and differentiation of T_{reg} cells in the thymus[5–11]. IL-2Rβ and γ_c are shared with the IL-15 receptor, whose signaling can also contribute to the induction of Foxp3 expression[12]. IL-2, in cooperation with the cytokine TGF-β, is also required for extrathymic T_{reg} cell differentiation[13].

While the role of IL-2R signaling in the induction of Foxp3 expression and T_{reg} cell differentiation in the thymus is well established, the importance of IL-2R expression in mature T_{reg} cells is not well understood. Although deficiency in STAT5 abolishes Foxp3 expression, it can be restored by increased amounts of the anti-apoptotic molecule Bcl2. That finding raised the possibility that a chief role of IL-2 might be in the survival of differentiating T_{reg} cells or their precursors[14]. It has also been reported that ablation of the pro-apoptotic protein Bim can rescue T_{reg} cells or their precursors from apoptosis associated with deficiency in IL-2 or IL-2R and restore the number of T_{reg} cells, but it does not prevent fatal autoimmunity[15]. However, a profound effect of congenital deficiency in IL-2, Bcl2 and Bim on the differentiation and selection of T_{reg} cells and self-reactive effector T cells (T_{eff} cells) has confounded interpretation of that observation. Antibody-mediated neutralization of IL-2 in adult mice that have undergone removal of the thymus reduces the number of T_{reg} cells and Foxp3 expression in T_{reg} cells[16,17]. Thus, IL-2 supports stability of the T_{reg} cell lineage after differentiation[18,19]. However, expression of a transgene encoding IL-2Rβ exclusively in thymocytes has been reported to rescue *Il2rb*$^{-/-}$ mice from lethal autoimmune disease, which suggests that IL-2R expression is dispensable in peripheral T_{reg} cells[7,11]. Thus, a role for IL-2R expression and signaling in peripheral T_{reg} cells has remained uncertain. Hypothetically, a role for IL-2R in peripheral T_{reg} cells could be threefold: guidance for T_{reg} cells to sense their targets, which are activated self-reactive T cells that serve as a source of IL-2; T_{reg} cell–mediated deprivation of IL-2 as a mechanism of suppression; and cell-intrinsic IL-2 signaling in differentiated T_{reg} cells to support their maintenance, proliferation or function due to triggering of JAK–STAT5, PI3K–Akt or Ras–ERK signaling pathways. Previous studies have focused mainly on the induction or maintenance of Foxp3, while other aspects of IL-2R function have not been firmly established due to the aforementioned limitations.

Despite their considerable reliance on IL-2 for the maintenance of Foxp3 expression, T_{reg} cells are unable to produce IL-2. The reason for the inhibition of autologous activation of STAT5 in T_{reg} cells and the potential biological importance of this IL-2-based T_{reg} cell–T_{eff} cell

[1]Howard Hughes Medical Institute, Memorial Sloan Kettering Cancer Center, New York, New York, USA. [2]Immunology Program, Memorial Sloan Kettering Cancer Center, New York, New York, USA. [3]Immunology Discovery, Biogen, Cambridge, Massachusetts, USA. [4]Herbert Irving Comprehensive Cancer Center, Columbia University, New York, New York, USA. [5]Department of Pathology and Cell Biology, Columbia University, New York, New York, USA. [6]Department of Microbiology and Immunology, Columbia University, New York, New York, USA. [7]Nomis Foundation Laboratories for Immunobiology and Microbial Pathogenesis, The Salk Institute for Biological Studies, La Jolla, California, USA. [8]Institute for Medical Microbiology and Hygiene, University of Mainz Medical Centre, Mainz, Germany. [9]Present addresses: Biotechnology, AbbVie, North Chicago, Illinois, USA (A.K.K.), and Exploratory Biology, Juno Therapeutics, Seattle, Washington, USA (J.D.F.). [10]These authors contributed equally to this work. Correspondence should be addressed to J.D.F. (jason.fontenot@junotherapeutics.com) or A.Y.R. (rudenska@mskcc.org).

Received 9 December 2015; accepted 27 July 2016; published online 5 September 2016; doi:10.1038/ni.3540

regulatory loop also remain unknown. It has been suggested that repression of IL-2 is needed to maintain the 'unbound' state of high-affinity IL-2R on T_{reg} cells, and unbound IL-2R serves a key role in T_{reg} cell–mediated suppression by depriving T_{eff} cells of IL-2 (refs. 20–24); however, whether this mechanism has a non-redundant role in suppression *in vivo* is unknown. To address the role of IL-2R and downstream signaling pathways in differentiated T_{reg} cells, we ablated IL-2Rα, IL-2Rβ and STAT5 in Foxp3-expressing cells. By simultaneously inducing expression of an active form of STAT5, we assessed the differential requirements for IL-2R expression and IL-2 signaling in T_{reg} cell homeostasis versus T_{reg} cell suppressor activity.

RESULTS

IL-2R is indispensable for T_{reg} cell function

To definitively establish a role for IL-2R in T_{reg} cell function *in vivo*, we generated mice with T_{reg} cell–specific conditional knockout of IL-2Rβ by using Cre recombinase driven by the endogenous *Foxp3* locus (*Foxp3*^{Cre}) to delete *lox*P-flanked *Il2rb* alleles (*Il2rb*$^{fl/fl}$) in T_{reg} cells after Foxp3 was expressed. *Il2rb*$^{fl/fl}$*Foxp3*^{Cre} mice developed systemic fatal autoimmune inflammatory lesions and lymphoproliferation, albeit somewhat milder than that observed in mice with germline *Foxp3* deficiency[3] (**Fig. 1a–c**). The expression of IL-2Rβ and IL-2Rα was lower in *Il2rb*$^{fl/fl}$*Foxp3*^{Cre} peripheral T_{reg} cells than in their *Il2rb*$^{fl/wt}$*Foxp3*^{Cre} counterparts (**Fig. 1d**), and tyrosine-phosphorylation of STAT5 in response to IL-2 was lacking in *Il2rb*$^{fl/fl}$*Foxp3*^{Cre} peripheral T_{reg} cells (**Fig. 1e**). The frequency of Foxp3$^+$ cells among CD4$^+$ T cells and the expression of Foxp3 on a per-cell basis were both lower in *Il2rb*$^{fl/fl}$*Foxp3*^{Cre} mice than in *Il2rb*$^{fl/wt}$*Foxp3*^{Cre} mice (**Fig. 1f**). In healthy *Il2rb*$^{fl/fl}$*Foxp3*$^{Cre/wt}$ female mice, in which IL-2Rβ-sufficient T_{reg} cells and IL-2Rβ-deficient T_{reg} cells co-exist due to random inactivation of the X chromosome, IL-2Rβ-deficient T_{reg} cells were under-represented (**Fig. 1g,h**). It has been suggested that IL-2 is selectively required for the maintenance of CD62L^{hi}CD44^{lo} T_{reg} cells but is dispensable for CD62L^{lo}CD44^{hi} T_{reg} cells[25]. However, we found that the abundance of both CD62L^{hi}CD44^{lo} T_{reg} cells and CD62L^{lo}CD44^{hi} T_{reg} cells was significantly lower in the absence of IL-2Rβ than in its presence in healthy *Il2rb*$^{fl/fl}$*Foxp3*$^{Cre/wt}$ female mice (**Supplementary Fig. 1a**). In these mice, IL-2Rβ-deficient (*Il2rb*$^{fl/fl}$*Foxp3*$^{Cre/wt}$) T_{reg} cells had lower expression of Foxp3 and the T_{reg} cell 'signature' molecules IL-2Rα, CTLA-4, GITR and CD103 than that of IL-2Rβ-sufficient (*Il2rb*$^{fl/wt}$*Foxp3*$^{Cre/wt}$) T_{reg} cells regardless of their expression of CD62L and CD44 (**Fig. 1i,j** and **Supplementary Fig. 1a**). Although in diseased *Il2rb*$^{fl/fl}$*Foxp3*^{Cre} mice, the majority of T_{reg} cells were CD62L^{lo}CD44^{hi}, this was probably a consequence of severe inflammation, because the frequency of T_{reg} cells was also much lower in *Il2rb*$^{fl/fl}$*Foxp3*^{Cre} mice than in *Il2rb*$^{fl/wt}$*Foxp3*^{Cre} mice at sites at which CD62L^{lo}CD44^{hi} cells were prevalent—i.e., the small and large intestines (**Supplementary Fig. 1b**). Accordingly, the expression of many characteristic T_{reg} cell markers, except for CD25 and Foxp3, was upregulated as the result of T_{reg} cell activation in *Il2rb*$^{fl/fl}$*Foxp3*^{Cre} mice (**Supplementary Fig. 1c**). These observations suggested that both the CD62L^{hi}CD44^{lo} T_{reg} cell subset and the CD62L^{lo}CD44^{hi} T_{reg} cell subset, including those residing in non-lymphoid tissues, were dependent on IL-2, although under inflammatory conditions the latter was sustained to some extent by IL-2R-independent signals. Despite their upregulation of the expression of CTLA-4, GITR, the costimulatory receptor ICOS and CD103, the 'activated' IL-2Rβ-deficient T_{reg} cells from *Il2rb*$^{fl/fl}$*Foxp3*^{Cre} mice were still unable to control inflammation in the diseased mice and were not suppressive when transferred together with T_{eff} cells into lymphopenic recipients (data not shown).

Our findings raised the question whether ablation of IL-2Rα (which, in addition to facilitating IL-2 signaling, enables its sequestration from T_{eff} cells) would result in T_{reg} cell deficiency and disease similar to that of *Il2rb*$^{fl/fl}$*Foxp3*^{Cre} mice. Thus, we generated mice with a *lox*P-flanked *Il2ra* allele (J.D.F., data not shown) and induced its conditional ablation in T_{reg} cells by means similar to those described above. We found that T_{reg} cell–specific deficiency in IL-2Rα resulted in a disease with an early onset and severity similar to that observed after ablation of IL-2Rβ (**Supplementary Fig. 1d–f**). Of note, germline deficiency in either *Il2ra* or *Il2rb* in mice on the same C57BL6/J strain as that of our mice with conditional knockout resulted in a considerably less aggressive disease with a delayed onset (data not shown), probably due to the role of IL-2R signaling in T_{eff} cells. Our findings also indicated that IL-15 was unable to effectively compensate for the loss of IL-2 signaling in differentiated T_{reg} cells, because in *Il2ra*$^{fl/fl}$*Foxp3*^{Cre} mice, T_{reg} cells lacked only signaling via IL-2, whereas in *Il2rb*$^{fl/fl}$*Foxp3*^{Cre} mice, they lacked signaling via both IL-2 and IL-15, yet they were affected similarly. This was in contrast to T_{reg} cell differentiation in the thymus, in which IL-15 can contribute in part to Foxp3 induction[12].

Since IL-2R activates PI3K–Akt, MAPK, and JAK–STAT5 signaling pathways, we next sought to assess the role of STAT5 activation downstream of IL-2R signaling in T_{reg} cells. We found that ablation of STAT5 impaired T_{reg} cell function similarly to ablation of IL-2Rβ and that *Stat5a*$^{fl/fl}$*Stat5b*$^{fl/fl}$*Foxp3*^{Cre} mice were affected by fatal autoimmunity in a way similar to that of mice harboring IL-2R-deficient T_{reg} cells (**Supplementary Fig. 1g–k**). Thus, in agreement with IL-2-neutralization studies, these results indicated that IL-2R signaling was required for T_{reg} cell fitness in a cell-intrinsic manner.

Restoring STAT5 signaling in IL-2R-deficient T_{reg} cells

The findings reported above indicated that activation of STAT5 downstream of IL-2R was continuously required for T_{reg} cell function. However, the marked decrease in IL-2R expression observed in STAT5-deficient T_{reg} cells (**Supplementary Fig. 1g**) made it impossible to separate loss of STAT5 from impairment in all IL-2R functions (i.e., detection of IL-2, transduction of STAT5-dependent and STAT5-independent signals, and consumption and deprivation of IL-2) as a key contributor to the observed severe dysfunction of T_{reg} cells.

To address that major caveat and to understand the role of STAT5 versus that of IL-2R, we sought to determine whether expression of a gain-of-function form of STAT5b was able to restore T_{reg} cell function in the absence of IL-2R. A published study using a transgene encoding a constitutively active form of STAT5b (STAT5b-CA) driven by the proximal promoter of the gene encoding the kinase Lck in the absence of IL-2Rβ showed restoration of T_{reg} cell differentiation in the thymus but not rescue from lymphoproliferative syndrome[9]. However, the expression of this transgene early during thymopoiesis leads to leukemic lymphoproliferation, which complicated the interpretation of those findings. In addition, both the activity of the proximal *Lck* promoter and the expression of the transgene became lower over time in peripheral T cells in these mice[9]. Therefore, we generated a gene-targeted mouse strain using the *Rosa26* 'gene-trap' locus[26] in which a transgene encoding STAT5b-CA driven by a CAG promoter (chicken β-actin promoter with cytomegalovirus enhancers)[27] is preceded by a *lox*P-flanked STOP cassette (**Supplementary Fig. 2a**). In the resulting *Rosa26*^{Stat5bCA} mice, STAT5b-CA is expressed only when the *lox*P sites undergo Cre-mediated recombination. Introduction of the *Rosa26*^{Stat5bCA} allele into *Il2rb*$^{fl/fl}$*Foxp3*^{Cre} mice and the consequent expression of STAT5b-CA in IL-2Rβ-deficient T_{reg} cells rescued the mice from the systemic inflammation and early fatal disease (**Supplementary Fig. 2b**). In these mice, the frequency and

© 2016 Nature America, Inc. All rights reserved.

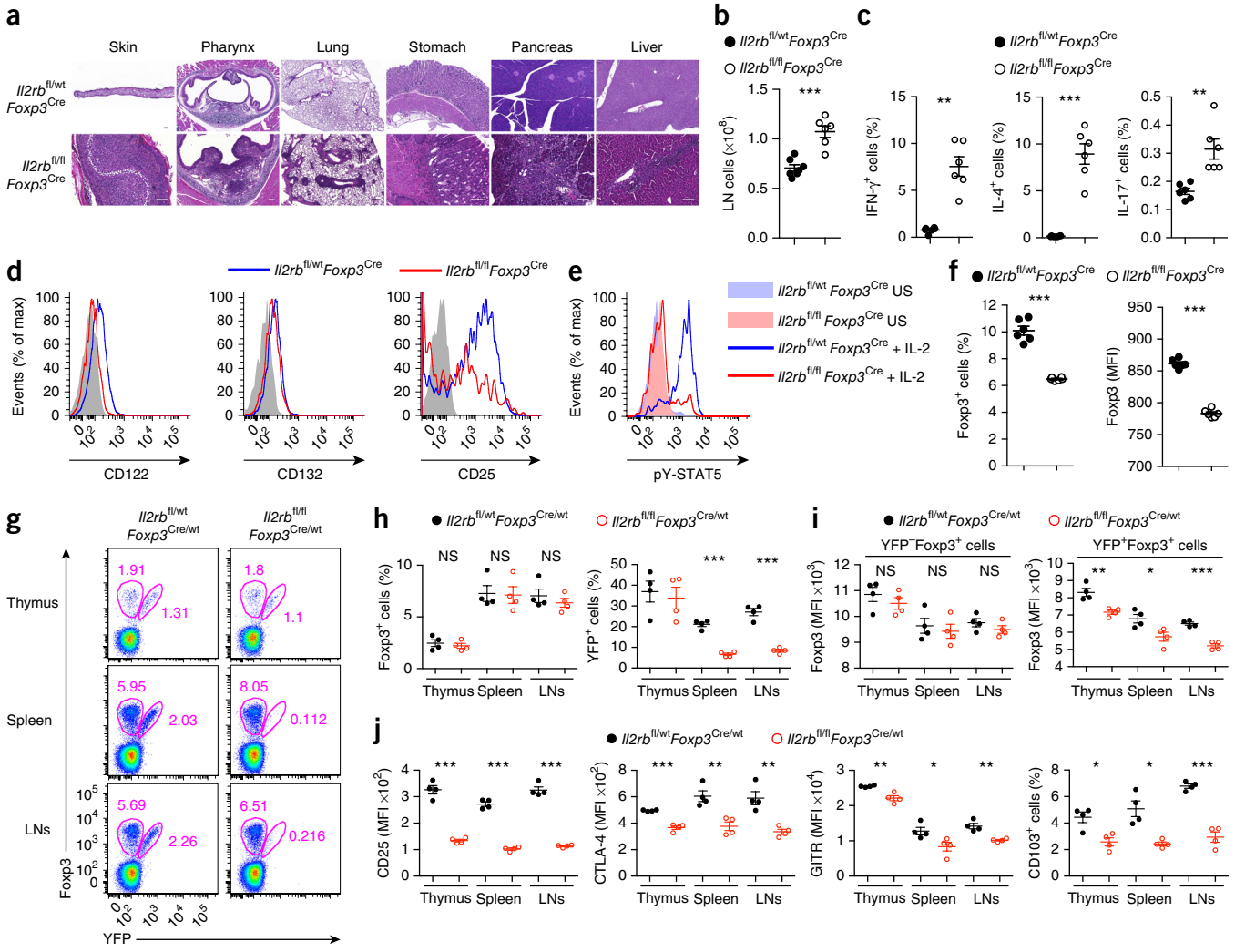

Figure 1 IL-2Rβ is indispensable for T_{reg} cell function. (**a**) Histopathology of various tissues (above images) from *Il2rb*$^{fl/wt}$*Foxp3*^{Cre} and *Il2rb*$^{fl/fl}$*Foxp3*^{Cre} mice (left margin). Scale bars, 100 μm. (**b**) LN cellularity of *Il2rb*$^{fl/wt}$*Foxp3*^{Cre} and *Il2rb*$^{fl/fl}$*Foxp3*^{Cre} mice (key). (**c**) Frequency of IFN-γ$^+$ cells (left), IL-4$^+$ cells (middle) and IL-17$^+$ cells (right) among splenic CD4$^+$Foxp3$^-$ cells stimulated for 5 h with antibody to the invariant signaling protein CD3ε and antibody to the co-receptor CD28. (**d**) Expression of the IL-2R subunits IL-2Rβ (CD122), γc (CD132) and IL-2Rα (CD25) by CD4$^+$Foxp3$^+$ cells from *Il2rb*$^{fl/wt}$*Foxp3*^{Cre} and *Il2rb*$^{fl/fl}$*Foxp3*^{Cre} mice (key); gray shaded curve, isotype-matched control antibody. (**e**) Intracellular tyrosine-phosphorylated STAT5 (pY-STAT5) in *Il2rb*$^{fl/wt}$*Foxp3*^{Cre} and *Il2rb*$^{fl/fl}$*Foxp3*^{Cre} T_{reg} cells left unstimulated (US) or stimulated *in vitro* for 20 min with recombinant mouse IL-2 (1,000 U/ml). (**f**) Frequency of Foxp3$^+$ (T_{reg}) cells among LN CD3$^+$CD4$^+$ cells (left) and Foxp3 expression by the CD3$^+$CD4$^+$ Foxp3$^+$ cells, presented as mean fluorescence intensity (MFI) (right). (**g**) Flow cytometry of gated CD3$^+$CD4$^+$ cells from the thymus, spleen and LNs (left margin) of healthy heterozygous female *Il2rb*$^{fl/wt}$*Foxp3*$^{Cre/wt}$ or *Il2rb*$^{fl/fl}$*Foxp3*$^{Cre/wt}$ mice (above plots). Numbers adjacent to outlined areas indicate percent cells with intracellular Foxp3 staining (T_{reg} cells) with (top right) or without (top left) expression of Cre (assessed as yellow fluorescent protein (YFP), which is fused to Cre in *Foxp3*^{Cre} mice). (**h**) Frequency of Foxp3$^+$ cells among CD3$^+$CD4$^+$ cells (left) and of YFP$^+$ (Cre-expressing) cells among Foxp3$^+$ cells (right) from organs of mice as in **g**. (**i**) Foxp3 expression in YFP$^-$Foxp3$^+$ cells (left) and YFP$^+$Foxp3$^+$ cells (right) from organs of mice as in **g**. (**j**) Expression of the markers IL-2Rα (CD25), CTLA-4, GITR and CD103 by YFP$^+$Foxp3$^+$ cells from organs of mice as in **g**, analyzed by flow cytometry. Each symbol (**b**,**c**,**f**,**h**–**j**) represents an individual mouse (among 3- to 5-week-old sex- and age-matched mice); small horizontal lines indicate the mean (± s.e.m.). NS, not significant ($P > 0.05$); *$P < 0.05$, **$P < 0.01$ and ***$P < 0.001$ (two-tailed unpaired Student's *t*-test). Data are representative of two experiments with more than five mice per group (**a**) or three experiments with more than ten mice per group (**d**,**e**,**g**) or are from one experiment representative of three independent experiments with similar results, with three or more mice per group in each (**b**,**c**,**f**,**h**–**j**).

number of T_{reg} cells were comparable to or even surpassed those in IL-2R-sufficient *Il2rb*$^{wt/wt}$*Foxp3*^{Cre} mice (**Fig. 2a**). Notably, the expression of IL-2Rα was higher in T_{reg} cells from *Rosa26*^{Stat5bCA}*Il2rb*$^{fl/fl}$*Foxp3*^{Cre} mice than in those from *Il2rb*$^{fl/fl}$*Foxp3*^{Cre} or *Il2rb*$^{wt/wt}$*Foxp3*^{Cre} mice, despite the absence of the IL-2Rβ chain (**Fig. 2a**), which suggested that the expression of IL-2Rα on T_{reg} cells was controlled mainly by STAT5-dependent signaling but not by STAT5-independent signaling. Notably, these IL-2Rβ-deficient T_{reg} cells with heightened IL-2Rα expression remained unresponsive to IL-2 (**Fig. 2b**).

The observed restoration of the suppressor function of IL-2Rβ-deficient T_{reg} cells and rescue from the early fatal disease via expression of STAT5b-CA raised the possibility that the reintroduced high levels of IL-2Rα were responsible for these effects. However, expression of STAT5b-CA similarly rescued *Il2ra*$^{fl/fl}$*Foxp3*^{Cre} mice from the early fatal disease (**Supplementary Fig. 2c**–**h**). Notably, although the impaired ability of T_{reg} cells to capture and consume IL-2 in both *Il2rb*$^{fl/fl}$*Foxp3*^{Cre} mice and *Il2ra*$^{fl/fl}$*Foxp3*^{Cre} mice was not 'rescued' via expression of STAT5b-CA (**Fig. 2c**), the reactivity of CD4$^+$ T cells was

© 2016 Nature America, Inc. All rights reserved.

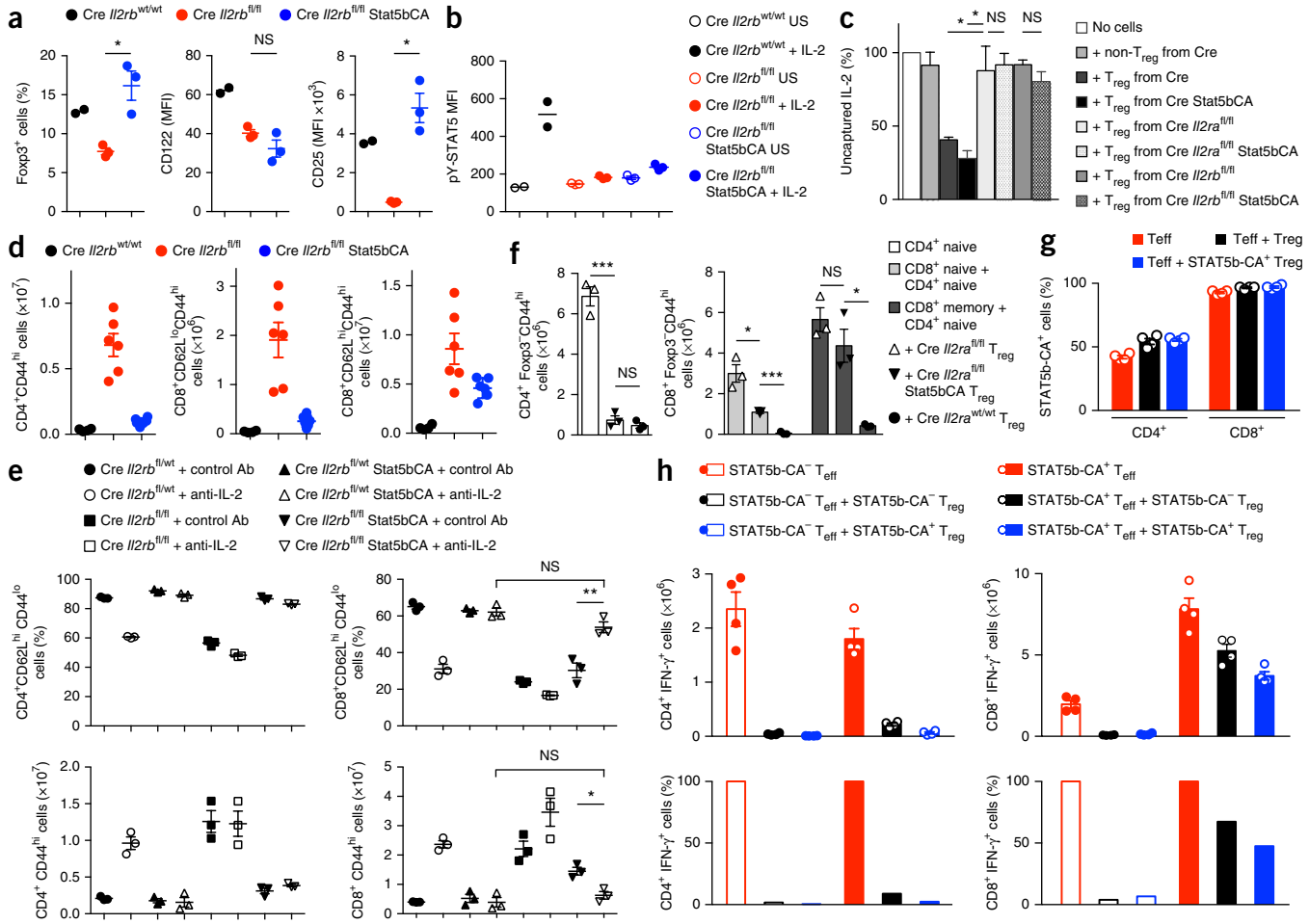

Figure 2 Restoration of the suppressor activity of IL-2R-deficient T_{reg} cells in the presence of an active form of STAT5. (**a**) Frequency of Foxp3$^+$ cells among CD3$^+$CD4$^+$ cells (left) and expression of CD122 and CD25 by CD3$^+$CD4$^+$Foxp3$^+$ cells (middle and right) from *Il2rb*$^{wt/wt}$*Foxp3*^{Cre} mice (Cre *Il2rb*$^{wt/wt}$), *Il2rb*$^{fl/fl}$*Foxp3*^{Cre} mice (Cre *Il2rb*$^{fl/fl}$) and *Rosa26*^{Stat5bCA}*Il2rb*$^{fl/fl}$*Foxp3*^{Cre} mice (Cre *Il2rb*$^{fl/fl}$Stat5bCA). (**b**) Quantification of intracellular tyrosine-phosphorylated STAT5 in LN T_{reg} cells obtained from mice as in **a** and left unstimulated or stimulated *in vitro* for 20 min with recombinant mouse IL-2 (1,000 U/ml). (**c**) Flow-cytometry-based bead-array analysis (*in vitro* IL-2 capture assay) of residual human IL-2 in the medium of non-T_{reg} cells sorted from *Foxp3*^{Cre} mice (+ non-T_{reg} from Cre) or T_{reg} cells sorted from mice as in **a** (key), assessed after culture for 2 h with recombinant human IL-2, or in medium of culture without cells (No cells). (**d**) Quantification of various subsets of CD4$^+$ or CD8$^+$ cells among CD3$^+$Foxp3$^-$ cells from the LNs of 2-week-old mice as in **a** (key). (**e**) Frequency of naive (CD62L^{hi}CD44^{lo}) T cells among CD3$^+$CD4$^+$Foxp3$^-$ and CD3$^+$CD8$^+$Foxp3$^-$ cells (top row) and quantification of CD44^{hi} activated CD3$^+$CD4$^+$Foxp3$^-$ and CD3$^+$CD8$^+$Foxp3$^-$ cells (bottom row) obtained from the LNs of mice as in **a** treated for 2 weeks (starting from day 5–7 after birth) with the control antibody IgG (+ control Ab) or with neutralizing antibody to IL-2 (+ anti-IL-2). (**f**) Quantification of CD4$^+$Foxp3$^-$CD44^{hi} and CD8$^+$Foxp3$^-$CD44^{hi} T cells in the LNs of T cell–deficient (*Tcrb*$^{-/-}$*Tcrd*$^{-/-}$) host mice 3 weeks after adoptive transfer of CD4$^+$Foxp3$^-$CD62L^{hi}CD44^{lo} (CD4$^+$ naive), CD8$^+$Foxp3$^-$CD62L^{hi}CD44^{lo} (CD8$^+$ naive) or CD8$^+$Foxp3$^-$CD62L^{hi}CD44^{hi} (CD8$^+$ memory) T cells (1×10^6 each) sorted from *Foxp3*^{Cre} mice (key, left), together with T_{reg} cells (2×10^5 cells) sorted from mice as in **a** (key, right). (**g**) Frequency of STAT5b-CA-expressing (STAT5b-CA$^+$) CD4$^+$ or CD8$^+$ T_{eff} cells among total CD4$^+$ or CD8$^+$ T_{eff} cells from *Tcrb*$^{-/-}$*Tcrd*$^{-/-}$ recipients 3 weeks after transfer of CD4$^+$Foxp3$^-$ or CD8$^+$Foxp3$^-$ T cells (1×10^6 cells each) sorted from *Rosa26*^{Stat5bCA}*Foxp3*^{Cre} mice and treated *in vitro* with TAT-Cre, without co-transfer of T_{reg} cells (T_{eff}) or with co-transfer of T_{reg} cells sorted from *Foxp3*^{Cre} mice (T_{eff} + T_{reg}) or *Rosa26*^{Stat5bCA}*Foxp3*^{Cre} mice (T_{eff} + STAT5b-CA$^+$ T_{reg}). (**h**) Quantification (top row) and frequency (bottom row) of IFN-γ$^+$ CD4$^+$ or CD8$^+$ T cells in recipients 3 weeks after transfer of CD4$^+$Foxp3$^-$ and CD8$^+$Foxp3$^-$ T cells sorted either from *Rosa26*^{wt}*Foxp3*^{Cre} mice (open bars) or *Rosa26*^{Stat5bCA}*Foxp3*^{Cre} mice (filled bars) and treated with TAT-Cre, without co-transfer of T_{reg} cells, or with co-transfer of 2×10^5 control T_{reg} cells sorted from *Foxp3*^{Cre} mice (+ Stat5b-CA$^-$ T_{reg}) or STAT5b-CA-expressing T_{reg} cells sorted from *Rosa26*^{Stat5bCA}*Foxp3*^{Cre} mice (+ Stat5b-CA$^+$ T_{reg}). Each symbol (**a**,**b**,**e**,**f**,**g**,**h**) represents an individual mouse; small horizontal lines (**a**,**b**,**e**) indicate the mean (± s.e.m.). $^*P < 0.05$, $^{**}P < 0.01$ and $^{***}P < 0.001$ (two-tailed unpaired Student's *t*-test). Data are from one experiment representative of three (**a**,**d**,**g**,**h**) or two (**b**,**c**,**e**,**f**) independent experiments with similar results, with two or more (**a**,**b**) or three or more (**c**,**d**,**e**,**f**,**g**,**h**) mice per group in each (mean + s.e.m. in **c**; mean ± s.e.m. in **f**,**g**,**h**).

fully controlled in these mice (**Fig. 2d** and **Supplementary Fig. 2d–h**). These results suggested that the ability to capture and compete for IL-2 was dispensable for T_{reg} cell–mediated suppression of CD4$^+$ T cell responses. In contrast, however, the population expansion of CD8$^+$ T cells, in particular that of activated CD62L^{hi}CD44^{hi} CD8$^+$ T cells, was restrained only marginally in these mice (**Fig. 2d** and **Supplementary Fig. 2f**,**h**). Although expansion of the CD8$^+$CD62L^{lo}CD44^{hi} subset was relatively well controlled, albeit not perfectly controlled, in neonatal mice (**Fig. 2d** and **Supplementary Fig. 2f**), this subset also gradually started to expand in these mice as early as 3 weeks after birth (**Supplementary Fig. 2i**). Although both *Rosa26*^{Stat5bCA}*Il2rb*$^{fl/fl}$*Foxp3*^{Cre} mice and *Rosa26*^{Stat5bCA}*Il2ra*$^{fl/fl}$*Foxp3*^{Cre} mice were rescued from premature death and showed substantially improved clinical status comparable to that of healthy controls, they gradually failed to

© 2016 Nature America, Inc. All rights reserved.

thrive and started to succumb to disease accompanied by massively expanded activated CD62L^{hi}CD44^{hi} and CD62L^{lo}CD44^{hi} CD8$^+$ T cell subsets in lymph nodes (LNs) and tissues by approximately 12 weeks of age (**Supplementary Fig. 2i**,**j**). These findings raised the possibility that IL-2 consumption by T_{reg} cells, while dispensable for the control of CD4$^+$ T cells, was important for the restraint of CD8$^+$ T cells.

T_{reg} cells suppress CD8$^+$ T cell responses via IL-2 depletion

To determine if the impairment in consumption of IL-2 by T_{reg} cells accounted for the proliferation of CD8$^+$ T cells in *Rosa26*^{Stat5bCA}*Il2rb*$^{fl/fl}$*Foxp3*^{Cre} mice, we administered IL-2-neutralizing antibodies to those mice starting from 5–7 d of age. As IL-2 supports the differentiation of T_{reg} cells in the thymus, neutralization of IL-2 reduced the frequency of T_{reg} cells in all groups of mice and induced immunoactivation in control *Il2rb*$^{fl/wt}$*Foxp3*^{Cre} mice (**Fig. 2e** and **Supplementary Fig. 3a**). In *Il2rb*$^{fl/fl}$*Foxp3*^{Cre} mice, which spontaneously developed disease, production of the T_H2 (T helper type 2) cytokines IL-4 and IL-13 by CD4$^+$ T cells was significantly reduced by neutralization of IL-2; however, the activation of CD4$^+$ and CD8$^+$ T cells was at best reduced only marginally or unaffected. In contrast, the activation and proliferation of CD8$^+$ T cells observed in *Rosa26*^{Stat5bCA}*Il2rb*$^{fl/fl}$*Foxp3*^{Cre} mice was almost completely suppressed by this treatment.

The relative reduction in the CD8$^+$CD62L^{lo}CD44^{hi} T cell subset and more pronounced proliferation of CD8$^+$CD62L^{hi}CD44^{hi} T cell subset in *Rosa26*^{Stat5bCA}*Il2rb*$^{fl/fl}$*Foxp3*^{Cre} and *Rosa26*^{Stat5bCA}*Il2ra*$^{fl/fl}$*Foxp3*^{Cre} mice raised the possibility that loss of IL-2-consumption by T_{reg} cells might selectively impair their suppression of the population expansion of memory CD8$^+$ T cells but not the recruitment of naive CD8$^+$ T cells into the effector-cell pool. We tested this idea by adoptive transfer of CD4$^+$ and CD8$^+$ cell subsets into lymphopenic recipients. Consistent with observations of *Foxp3*^{Cre} mice, the impaired suppression of the population expansion and activation of CD4$^+$ T cells by IL-2R-deficient T_{reg} cells was completely 'rescued' by STAT5b-CA; in contrast, their ability to suppress memory CD8$^+$ T cells was not restored, whereas suppression of the population expansion and activation of naive CD8$^+$ T cells was recovered only partially (**Fig. 2f**). Thus, IL-2 consumption by T_{reg} cells seemed to have a non-redundant role in suppressing the population expansion and activation of both the naive CD8$^+$ T cell subset and memory CD8$^+$ T cell subset, although this mechanism seemed to be particularly prominent in control of the latter subset.

Although the majority of activated CD8$^+$ T cells in *Il2rb*$^{fl/fl}$*Foxp3*^{Cre} and *Rosa26*^{Stat5bCA}*Il2rb*$^{fl/fl}$*Foxp3*^{Cre} mice did not have detectable expression of IL-2Rα (**Supplementary Fig. 3a**), these cells were able to activate STAT5 in response to IL-2, albeit to a lesser extent than that observed in cells expressing IL-2Rα (**Supplementary Fig. 3b**). A small proportion of activated CD4$^+$ T cells with undetectable IL-2Rα expression also responded to IL-2, but the majority of them did not (**Supplementary Fig. 3b**). naive T CD8$^+$ cells also responded to IL-2, while naive CD4$^+$ T cells did not (**Supplementary Fig. 3b**). Thus, both naive CD8$^+$ T cells and activated CD8$^+$ T cells seemed to be more sensitive to IL-2 than were CD4$^+$ T cells, and IL-2 consumption by T_{reg} cells might have markedly affected their activation. A corollary to that idea was that activation of STAT5 in CD8$^+$ T cells but not in CD4$^+$ T cells might render the former resistant to T_{reg} cell–mediated suppression. Thus, we tested the effect of STAT5 activation on the proliferation of CD4$^+$ or CD8$^+$ T cells in the presence of T_{reg} cells. For this purpose, we sorted CD4$^+$Foxp3$^-$ and CD8$^+$Foxp3$^-$ T cells from *Rosa26*^{Stat5bCA}*Foxp3*^{Cre} mice and induced expression of STAT5b-CA in these cells by treating them with recombinant Cre protein containing a membrane-permeable TAT peptide (trans-activating transcriptional activator from human immunodeficiency virus) (TAT-Cre). We adoptively transferred the treated cells into lymphopenic recipients with or without T_{reg} cells. Although treatment with TAT-Cre initially induced STAT5b-CA expression in approximately 30% of the treated CD4$^+$ T cells and CD8$^+$ T cells, more than 95% of CD8$^+$ T cells expressed STAT5b-CA 3 weeks after the cell transfer, whereas STAT5b-CA expressing CD4$^+$ T cells increased their frequency to only 40–50% (**Fig. 2g**). Notably, STAT5b-CA$^+$CD8$^+$ T cell populations robustly expanded in the presence of either control (*Il2ra*$^{wt/wt}$ *Foxp3*^{Cre}) T_{reg} cells or STAT5b-CA$^+$ T_{reg} cells (**Fig. 2g**,**h**). Although some degree of suppression of STAT5b-CA$^+$CD8$^+$ T cells by T_{reg} cells was still observed, it was very mild compared with the suppression of STAT5b-CA$^-$CD8$^+$ T cells (**Fig. 2h**). In contrast, the proliferation and cytokine production of activated CD4$^+$ T cells, regardless of the expression of STAT5b-CA, were well controlled by T_{reg} cells (**Fig. 2h**). These observations suggested that STAT5 activation in CD8$^+$ T cells prompted robust population expansion of cells and conferred pronounced resistance to T_{reg} cell–mediated suppression, but STAT5 activation in CD4$^+$ T cells did not. Consistent with those findings, gain-of-function experiments in which IL-2 was provided in the form of immunocomplexes of IL-2 and antibody to IL-2 showed population expansion of CD8$^+$ T cells and CD4$^+$ T_{reg} cells but not of CD4$^+$ T_{eff} cells[28]. Thus, while the ability to capture and compete for IL-2 was dispensable for T_{reg} cell–mediated suppression of CD4$^+$ T cell responses, this mode of suppression appeared to be essential for the control of CD8$^+$ T cells, which responded to excessive IL-2 more robustly than did CD4$^+$ T cells.

STAT5 activation in T_{reg} cells boosts immunosuppression

The lack of detectable STAT5 activation in response to IL-2 and of STAT5b-CA-driven population expansion of IL-2R-sufficient T_{reg} cells that escaped Cre-mediated recombination (counter-selection) in both *Rosa26*^{Stat5bCA}*Il2rb*$^{fl/fl}$*Foxp3*^{Cre} mice and *Rosa26*^{Stat5bCA}*Il2ra*$^{fl/fl}$*Foxp3*^{Cre} mice indicated that the expression of an active form of STAT5 relieved T_{reg} cells from their dependence on IL-2 signaling. This finding offered a unique opportunity to explore the biological importance of the aforementioned IL-2-dependent T_{reg} cell–T_{eff} cell regulatory network by uncoupling T_{reg} cell function from IL-2 production by T_{eff} cells. To address this issue, we generated *Rosa26*^{Stat5bCA}*Foxp3*$^{Cre–ERT2}$ mice, with tamoxifen-inducible expression of STAT5b-CA in differentiated T_{reg} cells (via the tamoxifen-sensitive estrogen receptor variant ERT2)[17]. Induction of STAT5b-CA expression in ~20–30% of T_{reg} cells by a single administration of tamoxifen was followed by their rapid increase in number at the expense of T_{reg} cells with a non-recombined *Rosa26*^{Stat5bCA} allele (**Supplementary Fig. 4a**,**b**). It was notable that these cells exhibited a highly diverse use of the T cell antigen receptor (TCR) β-chain variable region similar to that in *Rosa26*^{wt}*Foxp3*$^{Cre-ERT2}$ (control) mice (**Supplementary Fig. 4c**). The experimental *Rosa26*^{Stat5bCA}*Foxp3*$^{Cre-ERT2}$ mice remained healthy (**Supplementary Fig. 4d**,**e**). In these mice, the proliferated STAT5b-CA$^+$ T_{reg} cell population had larger amounts of Foxp3, CD25, CTLA-4 and GITR than those in STAT5b-CA$^-$ T_{reg} cells in tamoxifen-treated *Rosa26*^{wt}*Foxp3*$^{Cre-ERT2}$ mice and had a higher proportion of CD62L^{hi}CD44^{hi} cells than CD62L^{hi}CD44^{lo} cells (**Fig. 3a–d** and **Supplementary Fig. 4f**), indicative of a STAT5b-CA–imposed biasing of the T_{reg} cell population toward an activated state or a memory state. Consistent with those possibilities, surface expression of IL-7R, the activation marker KLRG1 and CD103 was higher in STAT5b-CA$^+$ T_{reg} cells in tamoxifen-treated *Rosa26*^{Stat5bCA}*Foxp3*$^{Cre-ERT2}$ mice than in STAT5b-CA$^-$ T_{reg} cells in tamoxifen-treated *Rosa26*^{wt}*Foxp3*$^{Cre-ERT2}$ mice (**Fig. 3d**). Notably, in the LNs and Peyer's patches, the number

© 2016 Nature America, Inc. All rights reserved.

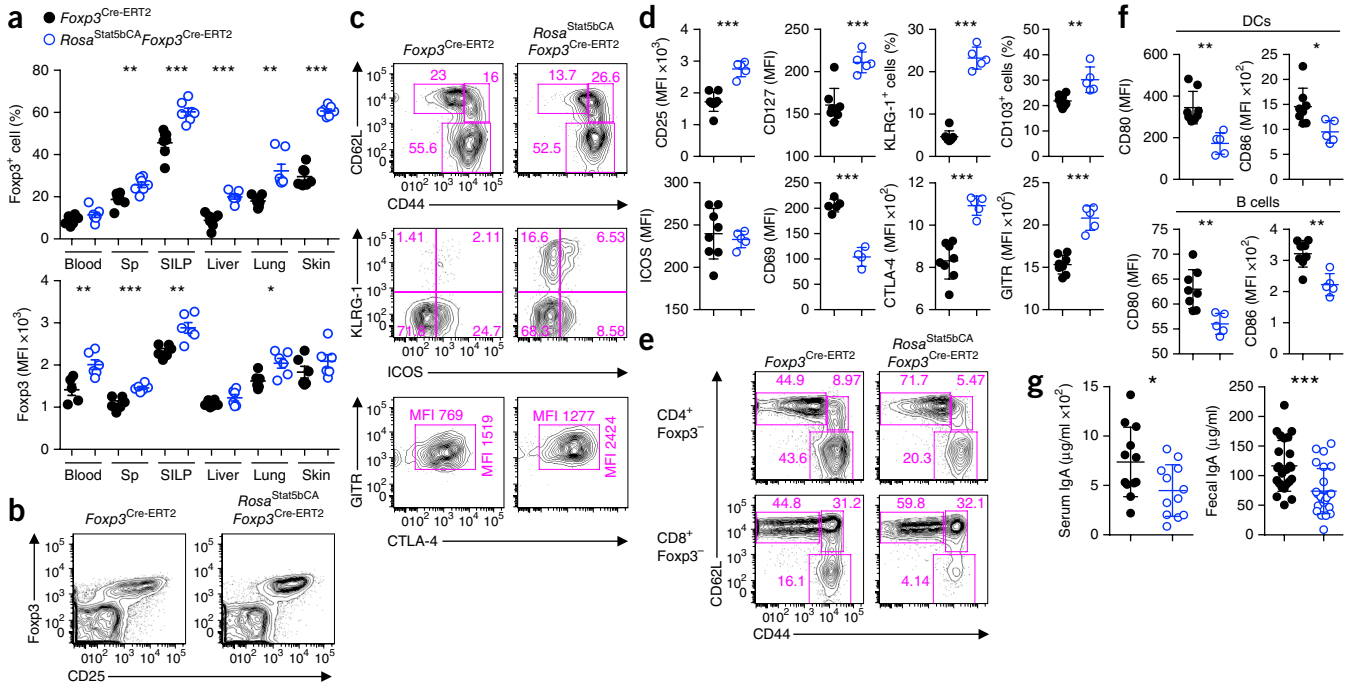

Figure 3 Increased proliferative and suppressor activity of T_{reg} cells expressing an active form of STAT5. (**a**) Frequency of Foxp3$^+$ cells among CD3$^+$CD4$^+$ cells (top) and expression of Foxp3 in CD3$^+$CD4$^+$Foxp3$^+$ cells (bottom) obtained from the blood, spleen (Sp), lamina propria of the small intestine (SILP), liver, lungs and skin (horizontal axes) of sex- and age-matched *Foxp3*$^{Cre\text{-}ERT2}$ and *Rosa26*^{Stat5bCA}*Foxp3*$^{Cre\text{-}ERT2}$ mice (key) 3 months after a single tamoxifen treatment, analyzed by flow cytometry. (**b**) Expression of Foxp3 and CD25 by splenic CD4$^+$ T cells from mice as in **a**. (**c**) Flow cytometry of splenic CD4$^+$Foxp3$^+$ T_{reg} cells from mice as in **a**. Numbers adjacent to outlined areas (top row) indicate percent CD62L^{hi}CD44^{lo} cells (top left), CD62L^{hi}CD44^{hi} cells (top right) or CD62L^{lo}CD44^{hi} cells (bottom); numbers in quadrants (middle row) indicate percent cells in each (throughout); numbers along margins of outlined areas (bottom row) indicate mean fluorescence intensity of CTLA-4 (top) or GITR (right). (**d**) Expression of various markers by splenic CD4$^+$Foxp3$^+$ T_{reg} cells from mice as in **a**, analyzed by flow cytometry. (**e**) Flow cytometry of splenic CD3$^+$CD4$^+$Foxp3$^-$ cells (top) and CD3$^+$CD8$^+$Foxp3$^-$ cells (bottom) from mice as in **a** (numbers in plots as in **c**, top). (**f**) Expression of CD80 and CD86 on DCs (CD11c$^+$MHCII^{hi}) and B cells (B220$^+$CD11c$^-$) in the LNs of mice as in **a**, analyzed by flow cytometry. (**g**) ELISA of serum and fecal IgA in mice as in **a**. Each symbol (**a**,**d**,**f**,**g**) represents an individual mouse; small horizontal lines indicate the mean (± s.e.m.). $^*P < 0.05$, $^{**}P < 0.01$ and $^{***}P < 0.001$ (two-tailed unpaired Student's *t*-test). Data are from one experiment representative of two independent experiments with similar results, with five or more mice per group in each (**a**,**d**,**f**,**g**) or are representative of three experiments with more than ten mice per group (**b**,**c**,**e**).

of T_{reg} cells did not increase after the administration of tamoxifen, despite the predominance of STAT5b-CA$^+$ T_{reg} cells in the former mice (**Supplementary Fig. 4b**,**g**); this suggested that T_{reg} cells with activated STAT5 'preferentially' distributed in non-lymphoid tissues. The abundance of CD8$^+$Foxp3$^+$ cells also increased after the induction of STAT5b-CA (**Supplementary Fig. 4h**). The 'autonomous' T_{reg} cells expressing active STAT5 showed heightened *in vitro* suppressor activity (**Supplementary Fig. 4i**) and effectively suppressed the basal state of activation and proliferative activity of CD4$^+$ and CD8$^+$ T cells *in vivo* as well, as indicated by the decreased number of Ki67$^+$ cells and CD62L^{lo}CD44^{hi} T_{eff} cells and much larger CD62L^{hi}CD44^{lo} naive T cell pool (**Fig. 3e** and **Supplementary Fig. 5a**,**b**). Accordingly, the production of pro-inflammatory cytokines, most prominently IL-4, by CD4$^+$ T cells and expression of the costimulatory molecules CD80 and CD86 by B cells and dendritic cells (DCs) were reduced after the administration of tamoxifen (**Fig. 3f** and **Supplementary Fig. 5c**). These results indicated that expression of STAT5b-CA conferred enhanced suppressor function to T_{reg} cells.

T_{reg} cells have been proposed to promote systemic responses of the T_H17 subset of helper T cells and class switching to immunoglobulin A (IgA) in the gut[29,30]. However, we found that serum and fecal IgA as well as T_H17 responses in secondary lymphoid organs were diminished rather than being increased in the presence of STAT5b-CA$^+$ T_{reg} cells (**Fig. 3g** and **Supplementary Fig. 5c**). Serum IgM and IgE also showed a tendency toward a decrease, but this was not statistically significant (**Supplementary Fig. 5d**). These results were in agreement with the increase in T_H17 responses and in both T_H2-type immunoglobulin class switching and T_H1-type immunoglobulin class switching observed upon acute ablation of T_{reg} cells[31].

Since altered intestinal immune responses have been linked to the promotion of colonic carcinogenesis, we explored an effect of a gain in T_{reg} cell suppressor function afforded by activated STAT5 in the *Apc*^{Min} model of colorectal cancer. Mice harboring the *Apc*^{Min} mutation develop multiple adenomatous polyps in the small intestine[32]. *Apc*^{Min}*Rosa26*^{Stat5bCA}*Foxp3*$^{Cre\text{-}ERT2}$ mice developed a number of polyps similar to or fewer than that of *Apc*^{Min}*Foxp3*$^{Cre\text{-}ERT2}$ mice, but the average polyp size was greater in *Apc*^{Min}*Rosa26*^{Stat5bCA}*Foxp3*$^{Cre\text{-}ERT2}$ mice than in *Apc*^{Min}*Foxp3*$^{Cre\text{-}ERT2}$ mice (**Supplementary Fig. 5e**). These results were consistent with the idea that suppression of inflammation by T_{reg} cells in tumor microenvironments promotes the growth of tumors once tumors or pre-cancerous lesions are already formed. However, the early stages of colonic carcinogenesis seemed to be not promoted but potentially suppressed by T_{reg} cells with augmented suppressor activity.

In addition to restraining the basal immunological reactivity in physiological settings and modulating colon-carcinoma development, 'autonomous' T_{reg} cells afforded superior protection against autoantigen-induced autoimmunity. We found that at 2–3 months after a single tamoxifen treatment, *Rosa26*^{Stat5bCA}*Foxp3*$^{Cre\text{-}ERT2}$ mice were very resistant to experimental autoimmune encephalomyelitis

© 2016 Nature America, Inc. All rights reserved.

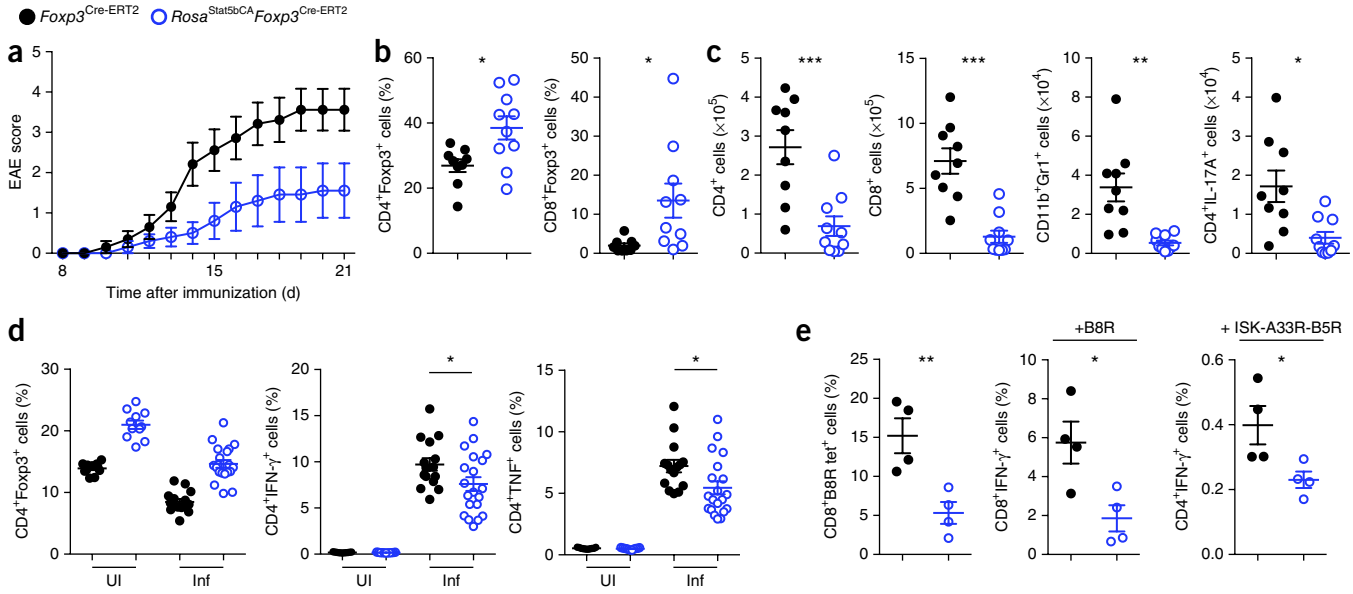

Figure 4 Potent suppressor function of T_{reg} cells expressing an active form of STAT5. (**a**) Experimental autoimmune encephalomyelitis (EAE) disease scores of sex- and age-matched *Foxp3*$^{Cre\text{-}ERT2}$ and *Rosa26*^{Stat5bCA}*Foxp3*$^{Cre\text{-}ERT2}$ mice ($n = 10$ per group) at various times after immunization. (**b**) Frequency of Foxp3$^+$ cells among brain-infiltrating CD3$^+$CD4$^+$ cells (left) and CD3$^+$CD8$^+$ cells (right) from mice as in **a** at day 22 after immunization, analyzed by flow cytometry. (**c**) Quantification of brain-infiltrating cells in mice as in **b**, analyzed by flow cytometry. (**d**) Frequency of Foxp3$^+$ cells among CD3$^+$CD4$^+$ cells (left) and of IFN-γ$^+$ cells (middle) or TNF$^+$ cells (right) among CD4$^+$TCRβ$^+$Foxp3$^-$ cells obtained from sex- and age-matched *Foxp3*$^{Cre\text{-}ERT2}$ and *Rosa26*^{Stat5bCA}*Foxp3*$^{Cre\text{-}ERT2}$ mice left uninfected (UI) or on day 8 after infection with *L. monocytogenes* (Inf), assessed by flow cytometry without re-stimulation (left) or after re-stimulation for 5 h *in vitro* with heat-killed *L. monocytogenes* in the presence of DCs (middle and right). (**e**) Frequency of CD8$^+$ T cells specific for the vaccinia virus peptide B8R (detected with H-2K^b–B8R tetramer (tet); left) and of IFN-γ$^+$ cells among CD8$^+$Foxp3$^-$ cells (middle) or CD4$^+$Foxp3$^-$ cells (right), in sex- and age-matched *Foxp3*$^{Cre\text{-}ERT2}$ and *Rosa26*^{Stat5bCA}*Foxp3*$^{Cre\text{-}ERT2}$ mice on day 8 after infection with non-replicating vaccinia virus, assessed by flow cytometry without re-stimulation (left) or after 5 h *in vitro* stimulation with the vaccinia virus peptide B8R (middle) or a mixture of three vaccinia-virus-specific peptides (ISK-A33R-B5R). Each symbol (**b**–**e**) represents an individual mouse; small horizontal lines indicate the mean (± s.e.m.). $^*P < 0.05$, $^{**}P < 0.01$ and $^{***}P < 0.001$ (two-tailed unpaired Student's *t*-test). Data are from one experiment representative of two independent experiments with similar results, with ten (**a**–**c**; mean ± s.e.m. in **a**) or four (**e**) mice per group in each (**a**–**c**,**e**) or are pooled from four independent experiments with $n = 11$ (UI), $n = 15$ (Inf, *Foxp3*$^{Cre\text{-}ERT2}$) or $n = 20$ (Inf, *Rosa26*^{Stat5bCA}*Foxp3*$^{Cre\text{-}ERT2}$) mice per group (**d**).

induced by immunization with myelin oligodendrocyte glycoprotein peptide in complete Freund's adjuvant (**Fig. 4a–c**). The frequency of CD4$^+$Foxp3$^+$ cells was significantly greater in the brain and spinal cord of these mice (**Fig. 4b**), and the infiltration of inflammatory cells, including neutrophils and IL-17-producing CD4$^+$ T_H17 cells, into these organs was significantly lower (**Fig. 4c**) than that of *Foxp3*$^{Cre\text{-}ERT2}$ mice. Pathogen-specific responses were also diminished in *Rosa26*^{Stat5bCA}*Foxp3*$^{Cre\text{-}ERT2}$ mice relative to those in *Foxp3*$^{Cre\text{-}ERT2}$ mice (also at 2–3 months after a single tamoxifen treatment). Although *Listeria-monocytogenes*-specific T_H1 responses were suppressed only modestly (**Fig. 4d**), vaccinia-virus-specific CD8$^+$ T cell responses were markedly reduced in the presence of STAT5b-CA$^+$ T_{reg} cells (**Fig. 4e**). Our observation of diminished responses to infectious agents and modulation of cancer progression might provide a rationale for why T_{reg} cells lack IL-2 production and autonomous activation of STAT5 and instead are reliant on activated T cells as a source of IL-2.

A distinct role for STAT5 activation in T_{reg} cells

Next we sought to address the question of how sustained STAT5 signaling might potentiate T_{reg} cells' suppressive ability. In genetic loss- and gain-of-function studies, STAT5 activity in T_{reg} cells correlated with their proliferative capacity and expression of IL-2Rα and Foxp3. However, the *in vitro* suppression assays reported above, as well as the diminished activation of the immune system in the LNs and Peyer's patches of *Rosa26*^{Stat5bCA}*Foxp3*$^{Cre\text{-}ERT2}$ mice, in which fewer T_{reg} cells were found than in *Foxp3*$^{Cre\text{-}ERT2}$ mice, suggested that the enhanced immunosuppression observed in *Rosa26*^{Stat5bCA}*Foxp3*$^{Cre\text{-}ERT2}$ mice was not simply due to a numerical increase of T_{reg} cells but that their suppressor activity on a per-cell basis was also augmented. It was also unlikely that mild upregulation of Foxp3 expression in the presence of STAT5b-CA could account for the increased suppressor activity of T_{reg} cells, as genome-wide binding of Foxp3 does not change after T_{reg} cells are activated, which leads to an increase in Foxp3 expression more pronounced than the one caused by STAT5b-CA[33]. The greater abundance of Foxp3 protein in STAT5b-CA$^+$ T_{reg} cells than in STAT5b-CA$^-$ T_{reg} cells was particularly noticeable in the CD25^{lo} T_{reg} cell subset (average difference in mean fluorescence intensity of Foxp3 in Foxp3$^+$ T_{reg} cells from *Rosa26*^{Stat5bCA}*Foxp3*$^{Cre\text{-}ERT2}$ mice versus that in those from *Foxp3*$^{Cre\text{-}ERT2}$ mice ($n = 6$): CD25^{hi} cells, 1.06-fold; CD25^{lo} cells, 1.36-fold; **Fig. 3b**), consistent with the observation that STAT5b-CA$^+$ T_{reg} cells were relieved from their dependence on IL-2. Nevertheless, STAT5b-CA$^+$ T_{reg} cells exhibited more potent suppressor function than that of CD25^{hi}Foxp3^{hi} T_{reg} cells from *Rosa26*^{wt}*Foxp3*$^{Cre\text{-}ERT2}$ (control) mice when transferred together with T_{eff} cells into lymphopenic recipients, despite comparably high expression of Foxp3 (data not shown). Thus, the enhanced suppressor activity of STAT5b-CA$^+$ T_{reg} cells was probably not due to the increase in Foxp3.

To gain insight into the potential mechanisms underlying the heightened suppressor function conferred by sustained activation of STAT5, we sorted mature T_{reg} cells from *Foxp3*$^{Cre\text{–}ERT2}$ and *Rosa26*^{Stat5bCA}*Foxp3*$^{Cre\text{-}ERT2}$ mice with comparable expression of Foxp3 and analyzed gene expression in these cells by high-throughput

© 2016 Nature America, Inc. All rights reserved.

sequencing technologies for cDNA (RNA-seq). While the gene-expression profiles of naive CD4$^+$ T cells from both groups of mice were nearly identical, gene expression in T_{reg} cells was markedly affected by the active form of STAT5 (**Fig. 5a** and **Supplementary Fig. 6a**). Among all genes expressed (~11,000) in either the T_{reg} cell populations or naive CD4$^+$ T cell populations analyzed, 342 genes

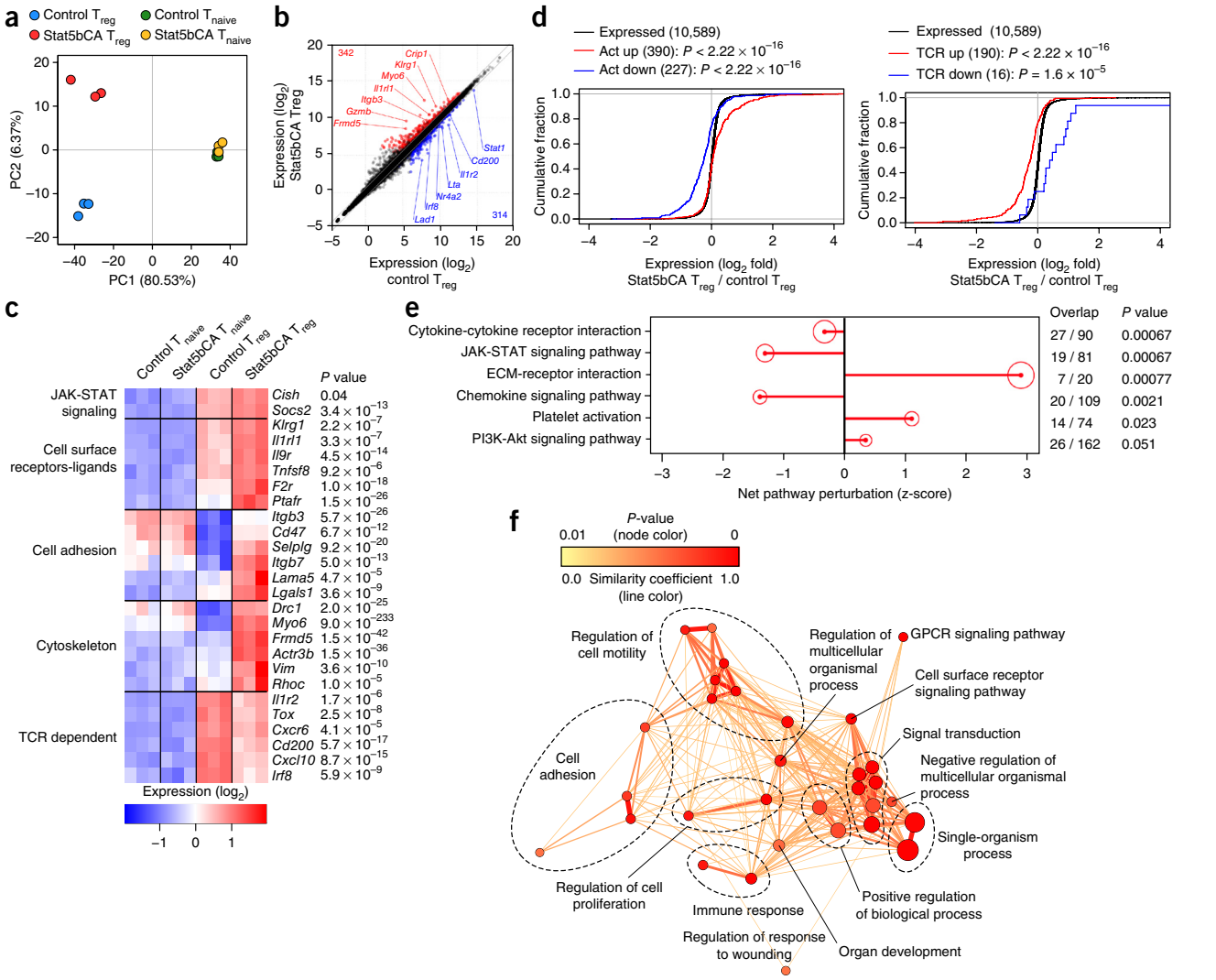

Figure 5 RNA-seq analysis of T_{reg} cells expressing an active form of STAT5. (**a**) Principal-component analysis of RNA-seq data sets of T_{reg} cells from *Foxp3*$^{Cre\text{-}ERT2}$ mice (Control T_{reg}), STAT5b-CA-expressing T_{reg} cells from *Rosa26*^{Stat5bCA}*Foxp3*$^{Cre\text{-}ERT2}$ mice (Stat5bCA T_{reg}), naive T cells from *Foxp3*$^{Cre\text{-}ERT2}$ mice (Control T_{naive}) or naive T cells from *Rosa26*^{Stat5bCA}*Foxp3*$^{Cre\text{-}ERT2}$ mice (Stat5bCA T_{naive}), assessed using the 15% of genes with the highest variance, presented as principal component 1 (PC1) and principal component 2 (PC2). Each symbol represents a single mouse. (**b**) Gene expression (log_2 normalized read count) in T_{reg} cells from *Foxp3*$^{Cre\text{-}ERT2}$ mice (Control T_{reg}) or STAT5b-CA-expressing T_{reg} cells from *Rosa26*^{Stat5bCA}*Foxp3*$^{Cre\text{-}ERT2}$ mice (Stat5bCA T_{reg}); diagonal lines indicate change in expression of at least 1.5-fold (top line) or 0.67-fold (bottom line); colors indicate significant (adjusted *P* value, ≤0.05) upregulation (of at least 1.5-fold; red) or downregulation (of at least 1.5-fold; blue) of expression above a minimal threshold based on the distribution of all genes; numbers in plots indicate total genes upregulated (red) or downregulated (blue). (**c**) Expression of selected genes (right margin) in cells as in **a** (three replicates per cell subset (columns)), grouped by product function (left margin); *P* values (far right), *Foxp3*$^{Cre\text{-}ERT2}$ T_{reg} cells versus STAT5b-CA-expressing T_{reg} cells. (**d**) Empirical cumulative distribution function for the change in expression (log_2 values) of all genes expressed in STAT5b-CA$^+$ T_{reg} cells (Expressed; change relative to that in *Foxp3*$^{Cre\text{-}ERT2}$ T_{reg} cells) and for subsets of genes upregulated (Act up) or downregulated (Act down) by inflammatory activation in T_{reg} cells[33] (left) or the subsets of genes upregulated (TCR up) or downregulated (TCR down) in a TCR-dependent manner in CD44^{hi} T_{reg} cells[34] (right). Numbers in parentheses (key) indicate total genes in each group. (**e**) Signaling-pathway-impact analysis of the pathways with the most significant enrichment for the expression of genes with related function from the Kyoto Encyclopedia of Genes and Genomes (left margin) showing enrichment among genes expressed differentially in STAT5b-CA$^+$ T_{reg} cells relative to their expression in *Foxp3*$^{Cre\text{-}ERT2}$ T_{reg} cells, presented as net pathway perturbation (status of pathway: activated (positive values) or inhibited (negative values)) based on activating or inhibitory relationships of genes expressed differentially in the pathway; circle size is proportional to the degree of enrichment); right margin (Overlap), genes in the pathway expressed differentially in STAT5b-CA$^+$ T_{reg} cells versus control *Foxp3*$^{Cre\text{-}ERT2}$ T_{reg} cells, divided by total genes in the pathway expressed either in STAT5b-CA$^+$ T_{reg} cells or *Foxp3*$^{Cre\text{-}ERT2}$ T_{reg} cells; far right, false-discovery-rate (FDR)-adjusted global *P* value (reflecting both enrichment and perturbation). (**f**) Network analysis of gene-ontology term enrichment among genes significantly upregulated in STAT5b-CA$^+$ T_{reg} cells relative to their expression in *Foxp3*$^{Cre\text{-}ERT2}$ T_{reg} cells; dashed outlines (added manually) indicate groups of similar gene-ontology terms (**Supplementary Table 1**); line thickness and color are proportional to the similarity coefficient between connected nodes; node color is proportional to the FDR-adjusted *P* value of the enrichment and node size is proportional to gene-set size.

© 2016 Nature America, Inc. All rights reserved.

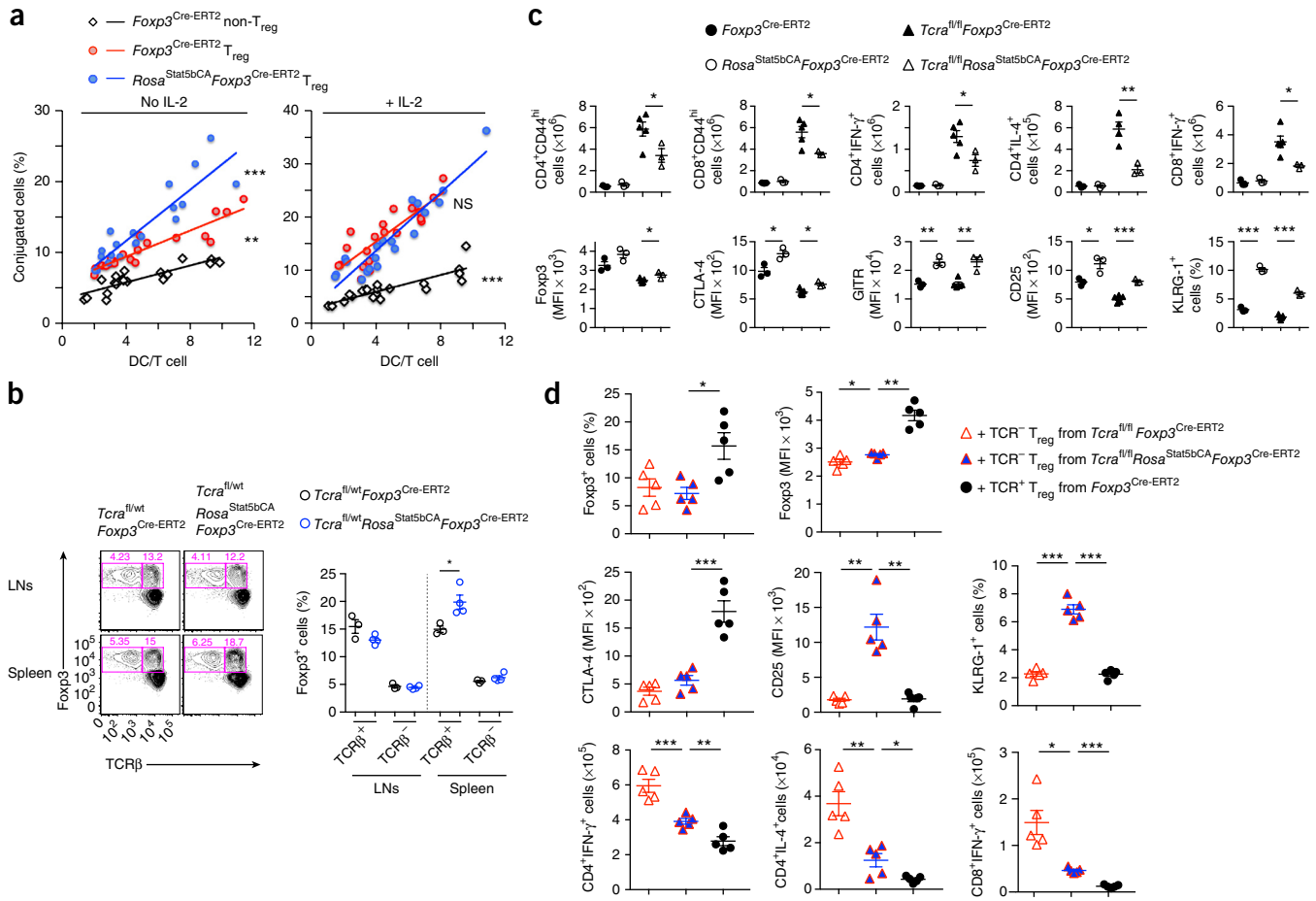

Figure 6 Augmented STAT5 signaling in T_{reg} cells increases the formation of conjugates of T_{reg} cells and DCs and potentiates suppressor function in a TCR-independent manner. (**a**) *In vitro* formation of conjugates of *Foxp3*$^{Cre\text{-}ERT2}$ non-T_{reg} cells or *Foxp3*$^{Cre\text{-}ERT2}$ or *Rosa26*^{Stat5bCA}*Foxp3*$^{Cre\text{-}ERT2}$ T_{reg} cells (key) (obtained from sex- and age-matched mice and labeled with the dye CFSE) and CD11c$^+$ DCs (obtained from C57BL/6J mice and labeled with the dye CellTrace Violet), assessed by flow cytometry after culture together for 720 min at various ratios (horizontal axes) in the absence (left) or presence (right) of recombinant mouse IL-2 (100 IU/ml), analyzed by flow cytometry; each symbol represents a single well. (**b**) Flow cytometry (left) of CD4$^+$ cells in the LNs and spleen of sex- and age-matched *Tcra*$^{fl/wt}$*Foxp3*$^{Cre\text{-}ERT2}$ or *Tcra*$^{fl/wt}$*Rosa26*^{Stat5bCA}*Foxp3*$^{Cre\text{-}ERT2}$ mice (above plots) treated for 2 weeks with tamoxifen. Numbers adjacent to outlined areas indicate percent Foxp3$^+$TCRβ$^-$ cells (top left) or Foxp3$^+$TCRβ$^+$ cells (top right). Right, summary of the frequency of TCR-sufficient (TCRβ$^+$) and TCR-deficient (TCRβ$^-$) Foxp3$^+$ cells among CD4$^+$ cells at left. (**c**) Frequency of CD44^{hi} (activated) T cells and cells positive for various pro-inflammatory cytokines in the LNs of sex- and age-matched *Foxp3*$^{Cre\text{-}ERT2}$, *Rosa26*^{Stat5bCA}*Foxp3*$^{Cre\text{-}ERT2}$, *Tcra*$^{fl/fl}$*Foxp3*$^{Cre\text{-}ERT2}$ and *Tcra*$^{fl/fl}$*Rosa26*^{Stat5bCA}*Foxp3*$^{Cre\text{-}ERT2}$ mice (key) treated with tamoxifen for 2 weeks (top row), and expression of Foxp3, CTLA-4, GITR, IL-2Rα (CD25) and KLRG1 in T_{reg} cells from the LNs of those mice (bottom row), analyzed by flow cytometry. (**d**) Frequency of T_{reg} cells and Foxp3 expression in T_{reg} cells (top row), expression of CTLA-4, IL-2Rα (CD25) and KLRG1 in T_{reg} cells (middle row) and quantification of cytokine-producing CD4$^+$ and CD8$^+$ T cells (bottom row) in the LNs of *Tcrb*$^{-/-}$*Tcrd*$^{-/-}$ recipient mice 3 weeks after transfer of wild-type CD4$^+$Foxp3$^-$ and CD8$^+$Foxp3$^-$ T cells (5×10^5 cells each) together with T_{reg} cells with TCR ablation (TCRβ^{lo}CD3^{lo}; TCR$^-$ T_{reg}) or TCR-sufficient T_{reg} cells (TCR$^+$ T_{reg}) (3×10^5 cells each) sorted from sex- and age-matched *Tcra*$^{fl/fl}$*Foxp3*$^{Cre\text{-}ERT2}$, *Tcra*$^{fl/fl}$*Rosa26*^{Stat5bCA}*Foxp3*$^{Cre\text{-}ERT2}$ or *Foxp3*$^{Cre\text{-}ERT}$ mice (key) treated for 2 weeks with tamoxifen, analyzed by flow cytometry. Each symbol (**b**–**d**) represents an individual mouse; small horizontal lines indicate the mean (± s.e.m.). $^*P < 0.05$, $^{**}P < 0.01$ and $^{***}P < 0.001$ (modified ANCOVA in Prism software (**a**) or two-tailed unpaired Student's *t*-test (**b**–**d**)). Data are from one experiment representative of three (**a**) or two (**b**,**d**) or four (**c**) independent experiments with similar results with three or more (**b**,**c**) or five or more (**d**) mice per group in each.

were upregulated and 314 genes were downregulated in STAT5b-CA$^+$ T_{reg} cells relative to their expression in STAT5b-CA$^-$ T_{reg} cells (**Fig. 5b** and **Supplementary Fig. 6b**). The gene set upregulated in STAT5b-CA$^+$ T_{reg} cells encoded various cell-surface molecules and receptors involved in cell adhesion, migration and cytoskeletal reorganization (**Fig. 5c**). Several genes that were upregulated or downregulated in STAT5b-CA$^-$ T_{reg} cells relative to their expression in naive T cells showed an opposite trend in STAT5b-CA$^+$ T_{reg} cells (**Fig. 5c**), which suggested that STAT5b-CA did not simply reinforce the T_{reg} cell signature. A published study has shown that exposure of T_{reg} cells to inflammation induced by transient depletion of T_{reg} cells leads to a marked change in their gene expression and a potent increase in their suppressor function[33]. Consistent with the heightened suppressor function of STAT5b-CA$^+$ T_{reg} cells, we found that the gene-expression changes in these cells conferred by the active form of STAT5 correlated with those found in highly activated T_{reg} cells in inflammatory settings (**Fig. 5d**). TCR signaling is required for the ability of T_{reg} cells to exert their suppressor function[34,35]. Thus, it was possible that the TCR- and STAT5-dependent signaling pathways in T_{reg} cells were acting on a largely overlapping set of genes whose expression they jointly regulated to potentiate the suppressor activity of T_{reg} cells. However, our analysis revealed that the gene set affected by the

© 2016 Nature America, Inc. All rights reserved.

active form of STAT5 was distinct from that expressed in T_{reg} cells in a TCR-dependent manner (**Fig. 5d**). Thus, both the TCR signaling pathway and STAT5 signaling pathway served an indispensable role in the suppressor activity of T_{reg} cells *in vivo* by controlling largely distinct sets of genes and probably distinct aspects of T_{reg} cell suppressor activity.

To better understand aspects of T_{reg} cell function potentiated by activation of STAT5, we performed analysis of signaling pathways and molecular-function enrichment. This revealed over-representation of gene sets encoding products involved in cell-cell and extracellular matrix interactions, cell adhesion and cellular locomotion among genes expressed differentially in STAT5b-CA$^+$ T_{reg} cells relative to their expression in STAT5b-CA$^-$ T_{reg} cells (**Fig. 5e**,**f** and **Supplementary Fig. 6c**). This result suggested that in T_{reg} cells, activation of STAT5 might potentiate their interactions with the target cells.

Since intravital imaging of T_{reg} cells *in vivo* has revealed their stable interactions with DCs[36], we assessed the potential effect of constitutively active STAT5 in T_{reg} cells on their ability to form conjugates with DCs *in vitro*. In agreement with the gene-set–enrichment analysis, we found that STAT5b-CA expression in T_{reg} cells promoted the formation of conjugates of T_{reg} cells and DCs (**Fig. 6a**). These enhanced interactions of STAT5b-CA$^+$ T_{reg} cells with DCs *in vitro* were consistent with the decreased expression of co-stimulatory molecules by DCs observed in tamoxifen-treated *Rosa26*^{Stat5bCA}*Foxp3*$^{Cre\text{-}ERT2}$ mice (**Fig. 3f**).

The findings reported above raised the question of whether activation of STAT5 can potentiate the suppressor function of T_{reg} cells in a TCR-independent manner. To investigate this, we analyzed *Rosa26*^{Stat5bCA}*Foxp3*$^{Cre\text{-}ERT2}$ mice with a *Tcra*^{fl} allele. Tamoxifen-inducible Cre-mediated ablation of *Tcra* (and thus the TCR) in T_{reg} cells is highly efficient in these mice and results in activation of the immune system that results from impaired suppressor function[34]. In heterozygous *Tcra*$^{fl/wt}$*Foxp3*$^{Cre\text{-}ERT2}$ mice, Cre-mediated recombination can theoretically result in ablation of the TCR in up to a half of T_{reg} cells due to allelic exclusion at the *Tcra* locus. We observed a small proportion of TCR-deficient T_{reg} cells in these mice after 2 weeks of tamoxifen administration (**Fig. 6b**). Although expression of the active form of STAT5 was observed in ~50% of TCR-sufficient and TCR-deficient T_{reg} cells in *Tcra*$^{fl/wt}$*Rosa26*^{Stat5bCA}*Foxp3*$^{Cre\text{-}ERT2}$ mice, the proportion of only TCR-sufficient STAT5b-CA$^+$ T_{reg} cells, not TCR-deficient STAT5b-CA$^+$ T_{reg} cells, was greater in these mice than in *Tcra*$^{fl/wt}$*Foxp3*$^{Cre\text{-}ERT2}$ mice (**Fig. 6b**). The marked increase in T cell activation and pro-inflammatory cytokine production was mitigated in part by expression of the active form of STAT5 in tamoxifen-treated *Tcra*$^{fl/fl}$*Rosa26*^{Stat5bCA}*Foxp3*$^{Cre\text{-}ERT2}$ mice (**Fig. 6c**). This partial recovery of T_{reg} cell suppressor function by the active form of STAT5 in T_{reg} cells that had undergone ablation of the TCR was also confirmed in experiments in which flow-cytometry-sorted TCR-deficient STAT5b-CA$^+$ T_{reg} cells and T_{eff} cells were adoptively transferred into lymphopenic recipients (**Fig. 6d**). Although the 'rescue' was incomplete, these results suggested that enhanced STAT5 signaling potentiated the suppressor activity of T_{reg} cells in the absence of contemporaneous TCR-dependent signals. Indeed, some features of T_{reg} cells that had been observed in TCR-sufficient STAT5b-CA$^+$ T_{reg} cells were still present in STAT5b-CA$^+$ T_{reg} cells that had undergone TCR ablation (**Fig. 6c**,**d**). However, we note that STAT5b-CA expression failed to restore suppressor function in *Tcra*$^{fl/fl}$*Rosa26*^{Stat5bCA}*Foxp3*^{Cre} mice in which TCR deletion occurred immediately after the induction of Foxp3 (data not shown). It has been shown that TCR signaling is required for the acquisition of an activated, antigen-experienced phenotype and suppressor function by T_{reg} cells[34]. Thus, our results suggested that activation of STAT5 potentiated TCR-independent suppressor function in mature T_{reg} cells that had already undergone TCR-dependent maturation. That observation is reminiscent of the sequential requirement for these two signals, via the TCR and IL-2R, in the differentiation of T_{reg} cells in the thymus, where STAT5 signaling promotes differentiation of T_{reg} cell precursors that have experienced permissive TCR signaling[37].

DISCUSSION

Published analysis of mice with germline deficiency in IL-2 and IL-2R subunits have demonstrated that IL-2 is a key cytokine required for the induction of Foxp3 expression and the differentiation of T_{reg} cells in the thymus[5–11]. Furthermore, antibody-mediated neutralization of IL-2 and provision of IL-2 in the form of immunocomplexes of IL-2 and antibody to IL-2, as well as genetic delineation of regulatory elements within the *Foxp3* locus, have revealed an important role for IL-2 in the maintenance of mature T_{reg} cells and in the stabilization of Foxp3 expression during their extrathymic differentiation[16,28,38]. Such findings have raised the question of whether IL-2R signaling can also directly promote the suppressor ability of T_{reg} cells and can therefore serve as a critical nexus linking the differentiation and maintenance of T_{reg} cells with their suppressor function. A published *in vitro* study has proposed a role for IL-2 signaling on the basis of indirect evidence[21]. In addition, consumption of IL-2 by T_{reg} cells has been suggested to serve an essential role in the suppressor function of T_{reg} cells by causing the death of activated CD4$^+$ T cells due to IL-2 deprivation[20–24]. On the other hand, other reports have suggested that IL-2R is dispensable for the ability of T_{reg} cells to suppress the proliferation of effector T cells[8,39]. Furthermore, the rescue of *Il2ra*$^{-/-}$ and *Il2rb*$^{-/-}$ mice from disease observed after adoptive transfer of wild-type T_{reg} cells suggested the existence of major mechanisms of T_{reg} cell–mediated suppression that are independent of IL-2-deprivation[6,7]. However, the last studies left open the major question of whether IL-2 consumption by T_{reg} cells is essential for the suppression of IL-2R-sufficient T_{eff} cells, since IL-2 is probably a main driver of autoimmune disease in the absence of functional T_{reg} cells.

A chief limiting factor in efforts to experimentally assess a role for IL-2R signaling in and IL-2 consumption by T_{reg} cells in their function *in vivo* has been the lack of adequate genetic tools. We addressed this issue through the conditional deletion of *Il2ra* and *Il2rb* alleles and ablation of the expression of these genes in T_{reg} cells in combination with induced expression of an active form of STAT5. These new genetic tools enabled us to unequivocally demonstrate a cell-intrinsic, essential role for IL-2R signaling not only in the maintenance of mature T_{reg} cells and their fitness but also in their suppressor function. Furthermore, we found that STAT5 deficiency in T_{reg} cells resulted in a similar loss of suppressor function and that expression of an active form of STAT5 rescued mice from the fatal disease that results from IL-2R deficiency. These results suggested a key role for IL-2R–STAT5 signaling in linking the differentiation and maintenance of T_{reg} cells and their function. STAT5 binds to the *Foxp3* promoter and the intronic *Foxp3* regulatory element CNS2 and is involved in the induction and maintenance of Foxp3 expression[38]. Complexes of the transcription factors Runx and CBFβ also bind to CNS2 and the *Foxp3* promoter and affect Foxp3 expression[40]. Although both CNS2-deficient T_{reg} cells and CBFβ-deficient T_{reg} cells do exhibit reduced Foxp3 expression resembling that of STAT5- or IL-2R-deficient T_{reg} cells, the impairment of suppressor function in the last is much more severe. Thus, the decrease in Foxp3 expression alone could not account for the severe loss of T_{reg} cell suppressor function in the absence of STAT5 or IL-2R. Indeed, our analysis of

© 2016 Nature America, Inc. All rights reserved.

gene expression and functional features conferred by expression of the active form of STAT5 pointed to a heightened ability of T_{reg} cells to bind to DCs and suppress their activation. Furthermore, expression of an active form of STAT5 partially 'rescues' the nearly complete loss of T_{reg} cell suppressor function in the absence of TCR signaling[34,35]. Such results might appear to be at odds with the published finding that a transgene encoding STAT5b-CA driven by the proximal *Lck* promoter and Eμ enhancer fails to curtail fatal lymphoproliferative disease in *Il2rb*$^{-/-}$ mice despite restoring Foxp3 expression and T_{reg} cell differentiation in the thymus[9]. However, the interpretation of the last result is problematic due to the massive population expansion of pre-leukemic T cells and B cells and reduced expression of the STAT5b-CA-encoding transgene in peripheral T_{reg} cells.

Our studies have demonstrated that depriving T_{eff} cells of IL-2 by T_{reg} cells was fully dispensable for the suppression of IL-2R-sufficient CD4$^+$ T cells, even though IL-2R signaling was required. However, IL-2R-dependent consumption of IL-2 by T_{reg} cells was indispensable for the suppression of CD8$^+$ T cell responses. The last, seemingly unexpected finding makes sense given the observed exquisite sensitivity of both naive CD8$^+$ T cells and activated CD8$^+$ T cells to IL-2-induced stimulation. Furthermore, IL-2 is produced upon activation of both naive CD4$^+$ T cells and CD8$^+$ T cells within hours of TCR engagement, in contrast to the production of effector cytokines such as IL-4 and IFN-γ, which requires the differentiation of naive T cells into T_{eff} cells on a much longer time scale[41]. Such distinguishing features provide a likely explanation for the need for a distinct mechanism for the control of CD8$^+$ T cell responses by T_{reg} cells through IL-2 consumption.

It has been suggested that sensing of local IL-2 production by T_{reg} cells enables 'licensing' of their suppressor function[21]. However, the 'rescue' of the suppression of CD4$^+$ T cell responses by IL-2R-deficient T_{reg} cells expressing an active form of STAT5 suggested that activated T_{reg} cells can suppress autoimmunity without identifying the cellular source of IL-2. Thus, while IL-2 is a booster for the suppressor function of T_{reg} cells, it might not have an indispensable role as a cue for specific targeting.

Genetically modified T cells are emerging as a potent means of therapy in some forms of cancer. The observed enhanced suppressor activity of T_{reg} cells expressing an active form of STAT5 and significantly reduced severity of organ-specific autoimmunity in their presence would suggest that such modification of T_{reg} cells might hold promise for the optimal design of T_{reg} cell–based therapies for a variety of autoimmune and inflammatory disorders and organ transplantation.

Our findings have highlighted a central role for IL-2R-signaling-driven activation of STAT5 in supporting and boosting the suppressor function of differentiated T_{reg} cells. In this context, it is noteworthy that although a *Foxp3* ortholog has not been identified in birds, CD4$^+$ T cell subsets with high expression of IL-2Rα have *in vitro* suppressor activity in chicken and ducks[42,43]. This suggests the importance of evolutionary conservation of IL-2Rα function in suppressive T cells.

METHODS

Methods and any associated references are available in the online version of the paper.

Accession codes. GEO: microarray data, GSE84553.

Note: Any Supplementary Information and Source Data files are available in the online version of the paper.

ACKNOWLEDGMENTS

We thank T. Kitamura (The University of Tokyo) for the mSTAT5b-CA vector (pMX-STAT5B(1*6)); K. Rajewsky (Max Delbrück Center) for the *Rosa26* construct; and L. Henninghausen (US National Institutes of Health) for *Stat5a-Stat5b*^{fl} mice. Supported by the Japan Society for the Promotion of Science, Strategic Young Researcher Overseas Visits Program for Accelerating Brain Circulation (T.C.), Lucille Castori Center for Microbes, Inflammation & Cancer (T.C.), the US National Institutes of Health Medical Scientist Training Program (T32GM07739 to the Weill Cornell/Rockefeller/Sloan Kettering Tri-Institutional MD-PhD Program, for A.G.L. and X.F.), the US National Institutes of Health (P30 CA008748 to Memorial Sloan Kettering Cancer Center Core Facilities; and R37 AI034206 to A.Y.R.), DFG Emmy Noether programme (G.G.), the Ludwig Center at Memorial Sloan Kettering Cancer Center (A.Y.R.), Hilton-Ludwig Cancer Prevention Initiative funded by the Conrad N. Hilton Foundation and Ludwig Cancer Research (A.Y.R.), and the Howard Hughes Medical Institute (A.Y.R.).

AUTHOR CONTRIBUTIONS

T.C., J.D.F. and A.Y.R. conceived of the project, designed the experiments and wrote and edited the manuscript.; T.C., A.K.K., A.G.L., X.F., Y.Z., G.G. and Y.F. conducted experiments; U.K. generated the *Il2rb*^{fl} allele; and J.D.F. generated the *Il2ra*^{fl} allele.

COMPETING FINANCIAL INTERESTS

The authors declare competing financial interests: details are available in the online version of the paper.

Reprints and permissions information is available online at http://www.nature.com/reprints/index.html.

1. Sakaguchi, S., Sakaguchi, N., Asano, M., Itoh, M. & Toda, M. Immunologic self-tolerance maintained by activated T cells expressing IL-2 receptor α-chains (CD25). Breakdown of a single mechanism of self-tolerance causes various autoimmune diseases. *J. Immunol.* **155**, 1151–1164 (1995).
2. Hori, S., Nomura, T. & Sakaguchi, S. Control of regulatory T cell development by the transcription factor Foxp3. *Science* **299**, 1057–1061 (2003).
3. Fontenot, J.D., Gavin, M.A. & Rudensky, A.Y. Foxp3 programs the development and function of CD4+CD25+ regulatory T cells. *Nat. Immunol.* **4**, 330–336 (2003).
4. Waldmann, T.A. The multi-subunit interleukin-2 receptor. *Annu. Rev. Biochem.* **58**, 875–911 (1989).
5. Furtado, G.C., Curotto de Lafaille, M.A., Kutchukhidze, N. & Lafaille, J.J. Interleukin 2 signaling is required for CD4+ regulatory T cell function. *J. Exp. Med.* **196**, 851–857 (2002).
6. Almeida, A.R., Legrand, N., Papiernik, M. & Freitas, A.A. Homeostasis of peripheral CD4+ T cells: IL-2R alpha and IL-2 shape a population of regulatory cells that controls CD4+ T cell numbers. *J. Immunol.* **169**, 4850–4860 (2002).
7. Malek, T.R., Yu, A., Vincek, V., Scibelli, P. & Kong, L. CD4 regulatory T cells prevent lethal autoimmunity in IL-2Rβ-deficient mice. Implications for the nonredundant function of IL-2. *Immunity* **17**, 167–178 (2002).
8. Fontenot, J.D., Rasmussen, J.P., Gavin, M.A. & Rudensky, A.Y. A function for interleukin 2 in Foxp3-expressing regulatory T cells. *Nat. Immunol.* **6**, 1142–1151 (2005).
9. Burchill, M.A., Yang, J., Vogtenhuber, C., Blazar, B.R. & Farrar, M.A. IL-2 receptor β-dependent STAT5 activation is required for the development of Foxp3+ regulatory T cells. *J. Immunol.* **178**, 280–290 (2007).
10. Yao, Z. *et al.* Nonredundant roles for Stat5a/b in directly regulating Foxp3. *Blood* **109**, 4368–4375 (2007).
11. Malek, T.R. & Bayer, A.L. Tolerance, not immunity, crucially depends on IL-2. *Nat. Rev. Immunol.* **4**, 665–674 (2004).
12. Vang, K.B. *et al.* IL-2, -7, and -15, but not thymic stromal lymphopoeitin, redundantly govern CD4+Foxp3+ regulatory T cell development. *J. Immunol.* **181**, 3285–3290 (2008).
13. Chen, W. *et al.* Conversion of peripheral CD4+CD25− naive T cells to CD4+CD25+ regulatory T cells by TGF-β induction of transcription factor Foxp3. *J. Exp. Med.* **198**, 1875–1886 (2003).
14. Malin, S. *et al.* Role of STAT5 in controlling cell survival and immunoglobulin gene recombination during pro-B cell development. *Nat. Immunol.* **11**, 171–179 (2010).
15. Barron, L. *et al.* Cutting edge: mechanisms of IL-2-dependent maintenance of functional regulatory T cells. *J. Immunol.* **185**, 6426–6430 (2010).
16. Setoguchi, R., Hori, S., Takahashi, T. & Sakaguchi, S. Homeostatic maintenance of natural Foxp3+ CD25+ CD4+ regulatory T cells by interleukin (IL)-2 and induction of autoimmune disease by IL-2 neutralization. *J. Exp. Med.* **201**, 723–735 (2005).
17. Rubtsov, Y.P. *et al.* Stability of the regulatory T cell lineage in vivo. *Science* **329**, 1667–1671 (2010).
18. Komatsu, N. *et al.* Heterogeneity of natural Foxp3+ T cells: a committed regulatory T-cell lineage and an uncommitted minor population retaining plasticity. *Proc. Natl. Acad. Sci. USA* **106**, 1903–1908 (2009).

© 2016 Nature America, Inc. All rights reserved.

19. Hori, S. Lineage stability and phenotypic plasticity of Foxp3$^+$ regulatory T cells. *Immunol. Rev.* **259**, 159–172 (2014).
20. Pandiyan, P., Zheng, L., Ishihara, S., Reed, J. & Lenardo, M.J. CD4$^+$CD25$^+$Foxp3$^+$ regulatory T cells induce cytokine deprivation-mediated apoptosis of effector CD4$^+$ T cells. *Nat. Immunol.* **8**, 1353–1362 (2007).
21. Thornton, A.M., Donovan, E.E., Piccirillo, C.A. & Shevach, E.M. Cutting edge: IL-2 is critically required for the in vitro activation of CD4$^+$CD25$^+$ T cell suppressor function. *J. Immunol.* **172**, 6519–6523 (2004).
22. Barthlott, T. *et al.* CD25$^+$CD4$^+$ T cells compete with naive CD4$^+$ T cells for IL-2 and exploit it for the induction of IL-10 production. *Int. Immunol.* **17**, 279–288 (2005).
23. Busse, D. *et al.* Competing feedback loops shape IL-2 signaling between helper and regulatory T lymphocytes in cellular microenvironments. *Proc. Natl. Acad. Sci. USA* **107**, 3058–3063 (2010).
24. Yamaguchi, T. *et al.* Construction of self-recognizing regulatory T cells from conventional T cells by controlling CTLA-4 and IL-2 expression. *Proc. Natl. Acad. Sci. USA* **110**, E2116–E2125 (2013).
25. Smigiel, K.S. *et al.* CCR7 provides localized access to IL-2 and defines homeostatically distinct regulatory T cell subsets. *J. Exp. Med.* **211**, 121–136 (2014).
26. Zambrowicz, B.P. *et al.* Disruption of overlapping transcripts in the ROSA beta geo 26 gene trap strain leads to widespread expression of β-galactosidase in mouse embryos and hematopoietic cells. *Proc. Natl. Acad. Sci. USA* **94**, 3789–3794 (1997).
27. Onishi, M. *et al.* Identification and characterization of a constitutively active STAT5 mutant that promotes cell proliferation. *Mol. Cell. Biol.* **18**, 3871–3879 (1998).
28. Boyman, O., Kovar, M., Rubinstein, M.P., Surh, C.D. & Sprent, J. Selective stimulation of T cell subsets with antibody-cytokine immune complexes. *Science* **311**, 1924–1927 (2006).
29. Chen, Y. *et al.* Foxp3$^+$ regulatory T cells promote T helper 17 cell development in vivo through regulation of interleukin-2. *Immunity* **34**, 409–421 (2011).
30. Cong, Y., Feng, T., Fujihashi, K., Schoeb, T.R. & Elson, C.O. A dominant, coordinated T regulatory cell-IgA response to the intestinal microbiota. *Proc. Natl. Acad. Sci. USA* **106**, 19256–19261 (2009).
31. Kim, J.M., Rasmussen, J.P. & Rudensky, A.Y. Regulatory T cells prevent catastrophic autoimmunity throughout the lifespan of mice. *Nat. Immunol.* **8**, 191–197 (2007).
32. Su, L.K. *et al.* Multiple intestinal neoplasia caused by a mutation in the murine homolog of the APC gene. *Science* **256**, 668–670 (1992).
33. Arvey, A. *et al.* Inflammation-induced repression of chromatin bound by the transcription factor Foxp3 in regulatory T cells. *Nat. Immunol.* **15**, 580–587 (2014).
34. Levine, A.G., Arvey, A., Jin, W. & Rudensky, A.Y. Continuous requirement for the TCR in regulatory T cell function. *Nat. Immunol.* **15**, 1070–1078 (2014).
35. Vahl, J.C. *et al.* Continuous T cell receptor signals maintain a functional regulatory T cell pool. *Immunity* **41**, 722–736 (2014).
36. Tadokoro, C.E. *et al.* Regulatory T cells inhibit stable contacts between CD4$^+$ T cells and dendritic cells in vivo. *J. Exp. Med.* **203**, 505–511 (2006).
37. Lio, C.W. & Hsieh, C.S. A two-step process for thymic regulatory T cell development. *Immunity* **28**, 100–111 (2008).
38. Feng, Y. *et al.* Control of the inheritance of regulatory T cell identity by a cis element in the Foxp3 locus. *Cell* **158**, 749–763 (2014).
39. Tran, D.Q. *et al.* Analysis of adhesion molecules, target cells, and role of IL-2 in human FOXP3$^+$ regulatory T cell suppressor function. *J. Immunol.* **182**, 2929–2938 (2009).
40. Rudra, D. *et al.* Runx-CBFbeta complexes control expression of the transcription factor Foxp3 in regulatory T cells. *Nat. Immunol.* **10**, 1170–1177 (2009).
41. Sojka, D.K., Bruniquel, D., Schwartz, R.H. & Singh, N.J. IL-2 secretion by CD4$^+$ T cells in vivo is rapid, transient, and influenced by TCR-specific competition. *J. Immunol.* **172**, 6136–6143 (2004).
42. Shanmugasundaram, R. & Selvaraj, R.K. Regulatory T cell properties of chicken CD4$^+$CD25$^+$ cells. *J. Immunol.* **186**, 1997–2002 (2011).
43. Andersen, K.G., Nissen, J.K. & Betz, A.G. Comparative genomics reveals key gain-of-function events in Foxp3 during regulatory T cell evolution. *Front. Immunol.* **3**, 113 (2012).

© 2016 Nature America, Inc. All rights reserved.

ONLINE METHODS

Mice. *Foxp3*^{Cre} and *Foxp3*$^{Cre–ERT2}$ mice were described previously[17,44]. *Il2ra*^{fl} mice were generated by J.D.F. *Stat5a/b*^{fl} mice were provided by L. Henninghausen. *Apc*^{Min} mice were purchased from the Jackson Laboratory. The targeting strategies to generate *Il2rb*^{fl} (generated by UK) and *Rosa26*^{Stat5bCA} alleles are shown in **Supplementary Figure 7**. *Tcra*^{fl} mice were described previously[34]. The experimental mice were either generated on or backcrossed onto a C57BL/6J (B6) background, bred and housed in the specific pathogen-free animal facility at Memorial Sloan Kettering Cancer Center. All animal experiments were approved by institutional animal care and use committee at Memorial Sloan Kettering Cancer Center and were performed in accordance with the institutional guidelines. For survival analysis, mice were monitored daily; unhealthy mice were euthanized once they were found lethargic and were counted as non-survivors. For tamoxifen treatment, tamoxifen (Sigma-Aldrich) was dissolved in olive oil at a concentration of 40 mg/ml. Mice were given oral gavage of 100 µl of tamoxifen emulsion per treatment. In experimental autoimmune encephalomyelitis and infection experiments, mice were challenged 2–3 months after a single gavage of tamoxifen and assessed as described previously[38].

Flow cytometry and cell sorting. Cells were stained with fluorescence-tagged antibodies purchased from eBioscience, BD Biosciences, Tonbo Bioscience or BioLegend (**Supplementary Table 2**) and analyzed using a BD LSR II flow cytometer. Flow cytometry data were analyzed using FlowJo software (TreeStar). For intracellular cytokine staining, cells were stimulated for 5 h with antibodies to CD3 and CD28 (5 µg/ml each) in the presence of brefeldin A or monensin, harvested and stained with eBioscience Fixation Permeabilization kit. For intracellular phosphorylated STAT5 staining, cells were stimulated with or without rmIL-2 for 20 min, fixed and permeabilized with 4% PFA followed by 90% methanol, and stained with anti-pY-STAT5 antibody (BD Biosciences). Cell sorting of Foxp3$^+$ and Foxp3$^-$ cells was performed based on YFP or GFP expression using a BD FACSAria II cell sorter.

***Listeria* and vaccinia infection.** Mice were given intravenous injection of *L. monocytogenes* (LM10403S; 2000 cells/mouse) into the tail vein on day 0 and analyzed on day 8. For the detection of *L. monocytogenes*–specific immune responses, splenic DCs from unchallenged B6 mice sorted using CD11c microbeads (Miltenyi) were cultured in wells of a 96-well U-bottom plate (2×10^4 cells/well) with heat-killed *L. monocytogenes* (2×10^7 cells/well) for 6 h before the analysis. The cells were then co-cultured with splenic T cells obtained from *L. monocytogenes*–infected mice (1×10^5 cells/well) for 5 h in the presence of brefeldin A, and cytokine-producing T cells were detected by flow cytometry. For vaccinia virus infection, mice were given intravenous injection of non-replicating virus (5×10^7 PFU/mouse) on day 0 and analyzed on day 8. Splenocytes were re-stimulated with various vaccinia-virus-derived antigenic peptides (1 µg/ml) for 5 h in the presence of brefeldin A, and cytokine-producing T cells were detected by flow cytometry.

***In vivo* IL-2 neutralization.** Mice were given intraperitoneal injection of a cocktail of two different anti-IL-2 monoclonal antibodies, JES6-1 and S4B6-1 (BioXcell), or isotype-matched control antibody (rat IgG2a, 2A3; BioXcell), 200 µg each, twice a week, starting from 5–7 d after birth.

TAT-Cre treatment of T cells. For the induction of STAT5b-CA expression in non-T_{reg} cells, 1×10^7 CD4$^+$Foxp3$^-$ or CD8$^+$Foxp3$^-$ T cells sorted from the LNs and spleens of *Foxp3*^{Cre} and *Rosa26*^{Stat5bCA}*Foxp3*^{Cre} mice were resuspended in 2 ml of serum-free RPMI medium containing a TAT-Cre recombinase (Millipore; 50 µg/ml) and incubated at 37 °C for 45 min. The cells were washed with RPMI containing 10% FCS, resuspended in PBS, and injected into T cell–deficient (*Tcrb*$^{-/-}$*Tcrd*$^{-/-}$) mice together with or without separately sorted T_{reg} cells for *in vivo* suppression assay.

***In vitro* IL-2 capture assay.** Pooled cells from LNs and spleens were depleted of B cells and accessary cells by panning and T cells were enriched. The cells were stained with anti-CD8 and anti-B220 (**Supplementary Table 2**), and CD4$^+$ T_{reg} cells were sorted on the basis of GFP (YFP) expression alone in CD8-negative population. The sorted cells were divided among eight wells of a 96-well V-bottomed plate (2×10^5 cells/well) in 25 µl RPMI medium (10% FCS) with or without increasing doses of recombinant human IL-2 (0.016 to 12 U/ml), followed by incubation for 2 h at 37 °C. Depletion of IL-2 from the medium was assessed with the BD Cytometric Bead Array and Human IL-2 Enhanced Sensitivity Flex Set according to the manufacturer's instructions (BD Biosciences).

***In vitro* T cell–DC conjugation assay.** T_{reg} cells and non-T_{reg} cells were sorted in the same manner as in the IL-2 capture assay. Splenic CD11c$^+$ DCs were isolated by magnetic-activated cell sorting from B6 mice given injection of Flt3L-secreting B16 melanoma cells. T_{reg} and non-T_{reg} cells were stained with CFSE. DCs were stained with CellTrace Violet (Molecular Probes). 1×10^4 T_{reg} or non-T_{reg} cells were cultured together with graded numbers of DCs (1×10^4 to 1×10^5) in a 96-well round-bottomed plate for 720 min in the presence or absence of rmIL-2 (100 IU/ml). Frequencies of T_{reg} cells conjugated with DCs (% CTV$^+$CFSE$^+$/CFSE$^+$) were analyzed by flow cytometry.

***In vitro* suppression assay.** Naive CD4$^+$ T cells (responder cells) and T_{reg} cells were purified by flow cytometry and stained with CellTrace Violet. 4×10^4 naive CD4$^+$ T cells were cultured with graded numbers of T_{reg} cells in the presence of 1×10^5 irradiated, T cell–depleted, CFSE-stained splenocytes and 1 µg/ml anti-CD3 (145-2C11, Bioxcell) in a 96-well round-bottom plate for 80 h. Cell proliferation of responder T cells and T_{reg} cells (live CFSE$^-$CD4$^+$Foxp3$^-$ and Foxp3$^+$) was determined by flow cytometry based on the dilution of fluorescence intensity of CellTrace Violet of the gated cells.

Measurement of serum and fecal immunoglobulin. Serum IgM, IgG1, IgG2a, IgG2b, IgG2c, IgG3 and IgA were measured by ELISA using SBA Clonotyping System (Southern Biotech). IgE ELISA was performed using biotinylated anti-IgE (R35-118, BD Biosciences) and HRP-conjugated streptavidin. For measurement of fecal IgA, fresh fecal pellets were collected and dissolved in extraction buffer (7 µl per mg pellet) containing 50 mM Tris-HCl, 150 mM NaCl, 0.5% NP-40, 1mM EDTA, 1 mM DTT, and protease inhibitor cocktail (Complete mini; Roche). Supernatants were collected after centrifugation, titrated, and IgA was measured by ELISA.

Statistical analysis for animal experiments. Each mouse was tagged with a unique identification number, and researchers were blinded to the genotypes of mice, except for adjustment of sample size included in a single experiment and after data analysis was completed. Wild-type mice with suspected congenital anomalies were excluded from the study. Cell samples that showed less than 70% cell vitality after preparation or after *in vitro* stimulation were excluded from the study. Statistical analyses were performed using Prism software with two-tailed unpaired Student's *t*-test. Welch's correction was applied when F-test was positive. *P* values of <0.05 were considered significant.

RNA sequencing. Male 8-week-old *Rosa26*^{Stat5bCA}*Foxp3*$^{Cre-ERT2}$ (STAT5b-CA) and *Foxp3*$^{Cre–ERT2}$ (control) mice, nine mice for each experimental group, received a single dose (4 mg) of tamoxifen by oral gavage 4 months before isolation. Splenic CD4$^+$Foxp3(YFP/GFP)$^+$GITR^{hi}CD25^{hi} T_{reg} and CD4$^+$Foxp3(YFP/GFP)$^-$CD62L^{hi}CD44^{lo} naive T cells were double sorted using a BD FACSAria II cell sorter, and a total of 12 samples were generated. Spleen T cell subsets isolated from three individual mice in the same experimental group were pooled into one biological replicate; three biological replicates were subjected to RNA-seq analysis for each experimental group. Total RNA was extracted and used for poly(A) selection and Illumina TruSeq paired-end library preparation following manufacturer's protocols. Samples were sequenced on the Illumina HiSeq 2500 to an average depth of 27.5×10^6 50-bp read pairs per sample. All samples were processed at a same time and sequenced on the same lane to avoid batch effects.

Read alignment and processing followed a method previously described[45]. Raw reads were trimmed using Trimmomatic v0.32 with standard settings to remove low-quality reads and adaptor contamination[46]. The trimmed reads were then aligned to the mouse genome (Ensembl assembly GRCm38) using TopHat2 v2.0.11 implementing Bowtie2 v2.2.2 with default settings. Read alignments were sorted with SAMtools v0.1.19 before being counted to genomic features using HTSeq v0.6.1p1. The overall read alignment

© 2016 Nature America, Inc. All rights reserved.
npg

doi:10.1038/ni.3540

rate across all samples was 74.5%. Differential gene expression was analyzed using DESeq2 1.6.3 in R (version 3.1.0)[47].

Bioinformatics analysis of RNA-seq. The distribution of read counts across all genes was bimodal. The assumption that this corresponded to 'expressed' and 'non-expressed' genes was supported by examination of marker genes known to be expressed or not expressed in T_{reg} cells and naive T cells. The local minimum between the two peaks was chosen to be the threshold for expression. Using this threshold of ~60 normalized reads, 10,589 of 39,179 genes were called as present. Genes significantly upregulated (342) or downregulated genes (314) in STAT5b-CA T_{reg} cells relative to their expression in control T_{reg} cells were defined as expressed genes with a change in expression of at least 1.5-fold or 0.67-fold, respectively, and a FDR-adjusted *P* value of ≤ 0.05.

'TCR-upregulated' (i.e., TCR-dependent) genes were defined as genes downregulated (a change in expression of at least 0.57-fold) in TCR-deficient relative to their expression inTCR-sufficient $CD44^{hi}$ T_{reg} cells, while 'TCR-downregulated' genes were upregulated (at least 1.75-fold; $P_{adj} \leq 0.001$) in TCR-deficient $CD44^{hi}$ T_{reg} cells (GSE61077)[34]. 'Activation-upregulated' genes were genes upregulated (twofold change; $P_{adj} \leq 0.01$) in T_{reg} cells from *Foxp3*^{DTR} mice recovering from transient depletion of T_{reg} cells (GSE55753)[33].

Signaling pathway impact analysis was performed using the R package of the same name[48]. Genes significantly up- and downregulated, and their changes in expression, were analyzed as one set for enrichment and perturbation of 90 *Mus musculus* KEGG (Kyoto Encyclopedia of Genes and Genomes) pathways accessed on 5 October 2015. The net pathway perturbation *z*-score was calculated using the observed net perturbation accumulation, and the mean and s.d. of the null distribution of net perturbation accumulations. Global *P* values were calculated using the normal inversion method with Bonferroni correction.

Biological-process (BP) gene-ontology (GO) term over-representation was calculated using BiNGO (v3.0.3)[49] in Cytoscape v3.2.1, employing the hypergeometric test and applying a significance cutoff of FDR-adjusted *P* value of ≤0.05. The 10,589 expressed genes were entered as the reference set, and the GO ontology and annotation files used were downloaded on 25 October 2015 (**Supplementary Table 1**). The output from BiNGO was imported into EnrichmentMap (v2.0.1)[50] in Cytoscape to cluster redundant GO terms and visualize the results. An EnrichmentMap was generated using a Jaccard similarity coefficient cutoff of 0.2, a *P*-value cutoff of 0.001, an FDR-adjusted cutoff of 0.005, and exclusion of gene sets with fewer than ten genes. The network was visualized using the default 'Prefuse Force-Directed Layout' in Cytoscape with default settings and 500 iterations. Groups of similar GO terms were manually circled.

44. Rubtsov, Y.P. *et al.* Regulatory T cell-derived interleukin-10 limits inflammation at environmental interfaces. *Immunity* **28**, 546–558 (2008).
45. Anders, S. *et al.* Count-based differential expression analysis of RNA sequencing data using R and Bioconductor. *Nat. Protoc.* **8**, 1765–1786 (2013).
46. Bolger, A.M., Lohse, M. & Usadel, B. Trimmomatic: a flexible trimmer for Illumina sequence data. *Bioinformatics* **30**, 2114–2120 (2014).
47. Love, M.I., Huber, W. & Anders, S. Moderated estimation of fold change and dispersion for RNA-seq data with DESeq2. *Genome Biol.* **15**, 550 (2014).
48. Tarca, A.L. *et al.* A novel signaling pathway impact analysis. *Bioinformatics* **25**, 75–82 (2009).
49. Maere, S., Heymans, K. & Kuiper, M. BiNGO: a Cytoscape plugin to assess overrepresentation of gene ontology categories in biological networks. *Bioinformatics* **21**, 3448–3449 (2005).
50. Merico, D., Isserlin, R., Stueker, O., Emili, A. & Bader, G.D. Enrichment map: a network-based method for gene-set enrichment visualization and interpretation. *PLoS One* **5**, e13984 (2010).

© 2016 Nature America, Inc. All rights reserved.